Chlorine Oxide Radicals ClO_x ($x = 1-4$) Studied by Matrix Isolation Spectroscopy

Rodion Kopitzky,[a] Hinrich Grothe,[b] and Helge Willner*[a]

Abstract: Low pressure flash thermolysis of different precursor molecules containing -ClO, -ClO_3 or -$OClO_3$ yield, when highly diluted in Ne or O_2 and subsequent quenching of the products in a matrix at 5 or 15 K, ClO_x ($x = 1, 3, 4$) radicals, respectively. If Ne or O_2 gas is directed over solid ClO_2 at $-120\,^{\circ}C$ and the resulting gas mixtures are immediately deposited as a matrix, a high fraction of $(OClO)_2$ is trapped. This enables recording of IR and UV spectra of weakly bonded $(OClO)_2$ dimers and detailled studying of their photochemistry. For Ne or O_2 matrix isolated ClO radicals the vibrational wavenumbers and electronic transitions are only slightly affected compared with the gas phase. In this study strong evidence is found for long lived ClO in the electronically excited $^2\Pi_{1/2}$ state. A comprehensive IR study of Ne matrix isolated ClO_3 (fundamentals at 1081, 905, 567, 476 cm^{-1}) yield i) a reliable force field; ii) a OClO bond angle of $\alpha_e = 113.8 \pm 1^{\circ}$ and iii) a ClO bond length of 148.5 ± 2 pm in agreement with predicted data from quantum chemical calculations. The UV/Vis spectrum of ClO_3 isolated in a Ne matrix (λ_{max} at 32100 and 23150 cm^{-1}) agrees well with the photoelectron spectrum of ClO_3^- and theoretical predictions. The origin of the structured high energy absorption is at 22696 cm^{-1} and three fundamentals (794, 498, 280 cm^{-1}) are detected in the $C\,^2E$ state. By photolysis of ClO_3 with visible light the complex $ClO \cdot O_2$ with ClO in the $^2\Pi_{1/2}$ state is formed. In an extended spectroscopic study of the elusive ClO_4 radical, isolated in a Ne or O_2 matrix, three additional IR bands, a complete UV spectrum and a strong interaction with O_2 are found. This leads to the conclusion that ClO_4 exhibits C_{2v} or C_s symmetry with a shallow potential minimum and forms with O_2 the previously unknown peroxy radical O_3ClO-O_2. All these results are discussed in the context of recent developments in the chemistry and spectroscopy of the important and interesting ClO_x ($x = 1-4$) family of radicals.

Keywords: chlorine compounds · matrix isolation · radical reactions · UV/Vis spectroscopy · vibrational spectroscopy

Introduction

Binary chlorine oxides Cl_xO_y ($x = 1, 2$; $y = 1-7$) are very important chemical species since they are involved in many reactions of industrial, environmental or academic interest. Due to the environmental role of the mononuclear radicals ClO_x ($x = 1-4$), especially in their involvement in ozone-depletion mechanisms and the formation of reactive intermediates, knowledge of these radicals has increased rapidly in recent years.[1]

[a] Prof. Dr. H. Willner, Dr. R. Kopitzky
Fakultät 4, Anorganische Chemie
Gerhard-Mercator Universität Duisburg
Lotharstrasse 1, 47048 Duisburg (Germany)
Fax: (+49) 203-379-2231
E-mail: willner@uni-duisburg.de

[b] Dr. H. Grothe
Institut für Materialchemie, Technische Universität Wien
Veterinärplatz 1, Trakt GA, 1210 Wien (Austria)
Fax: (+43) 1-25077-3890
E-mail: hgrothe@mail.zserv.tuwien.ac.at

The principal objective of this study is to review the recent developments in the chemistry and spectroscopy of the important and interesting ClO_x ($x = 1-4$) family of radicals and to report on new experimental results to complement our previous matrix studies on ClO_3[2] and ClO_4[3] radicals and the dimers of ClO[4] and OClO.[5]

Within the family of ClO_x radicals ($x = 1-4$), chlorine dioxide is the most established species, because it has been known for more than 180 years.[6–10] Chlorine dioxide is the only metastable chlorine oxide radical under normal conditions and is also of commercial interest. Its main uses are in the food industries, pulp bleaching in the paper industry, and water purification.[11] In the latter case, smaller amounts of chlorinated organic products are formed than by water treatment with chlorine or hypochlorite. There are several routes for the synthesis of OClO that involve the reduction of chlorates or the oxidation of chlorites [Eqs. (1), (2)].

$$2\,ClO_3^- + SO_2 \rightarrow 2\,ClO_2 + SO_4^{2-} \quad (1)$$

$$2\,ClO_2^- + Cl_2 \rightarrow 2\,ClO_2 + 2\,Cl^- \quad (2)$$

  0947-6539/02/0824-5601 $ 20.00+.50/0

Pure chlorine dioxide is potentially explosive. It can be handled safely as a diluted gas[12] (partial pressure up to 400 mbar, temperature below 303 K) or in aqueous solutions. The yellow paramagnetic gas (b.p. 11 °C) crystallizes at −59 °C and the yellow solid becomes diamagnetic at −84 °C.[13] The weakly bound dimers in the solid state have been structurally characterized,[13, 14] studied in the matrix by IR spectroscopy[5] and are the subject of theoretical calculations.[15] Scrambling of oxygen atoms between the isotopomers $Cl^{16}O_2$ and $Cl^{18}O_2$ occurs in the liquid state, presumably by dimer formation.[16]

For more than 15 years OClO has become an environmental product which can be observed in the stratosphere over the polar regions during spring time, where it is formed for example by the reaction of ClO with BrO.[1] This unexpected occurrence has gained further interest in OClO. Its properties have been studied extensively, including the microwave,[17, 18] millimeter and submillimeter wave,[19] high-resolution FTIR,[20–22] UV/Vis,[23, 24] photoelectron,[25] and photoion mass spectra[26, 27] and its photochemistry.[28, 29] Photofragmentation of OClO in the gas phase leads to ClO+O or to Cl+O_2, but the molar ratio of both channels is still under discussion.[29–35] Photolysis of matrix isolated OClO at temperatures below 100 K causes isomerization into ClOO.[5, 31, 36, 37] Both endothermic isomers, ClOO and OClO, are of comparable thermodynamic stability,[38–41] but ClOO is a short lived species as a result of its low Cl−O_2 bond energy of only 20 kJ mol^{-1}.[29] In contrast, organic peroxy radicals R-O_2 are of much higher stability, for example 150 kJ mol^{-1} for Et-OO or *t*Bu-OO.[42]

Transient ClO radicals have been first identified in studies about the photochemistry of Cl_2O and OClO as well as in the thermal and photochemical reactions of ozone with chlorine atoms.[43–58] Subsequent introduction of flash-photolysis techniques[59–61] has allowed investigation of the UV spectrum of ClO and its kinetics.[62–70] It should be noted that Bodenstein and Schumacher studied the kinetics of the reaction between ozone and chlorine atoms first,[49, 50] which has become very important in stratospheric chemistry. Ozone depletion processes in the stratosphere induced by chlorine atom release from halocarbons, as claimed by Rowland and Molina in 1974,[71] have increased the interest in halogen-oxygen chemistry. For the annual strong ozone depletion in the stratosphere over the polar regions, a catalytic cycle [Eqs. (3) – (5)] has been suggested.[72]

$$2\,O_3 + 2\,Cl \rightarrow 2\,ClO + 2\,O_2 \quad (3)$$

$$2\,ClO + M \rightarrow Cl_2O_2 + M \quad (4)$$

$$Cl_2O_2 + h\nu \rightarrow O_2 + 2\,Cl \quad (5)$$

$$2\,O_3 + h\nu \rightarrow 3\,O_2 \quad \Sigma(3)-(5)$$

Meanwhile the discussion concerning the photochemical cross section of Cl_2O_2 seems to be finished, since in the cycle mentioned above the contribution of BrOOCl was taken into account.[73, 74] Previously found discrepancies in the chlorine budget in the (lower and middle) stratosphere seem to be ruled out by more recent measurements.[75–79] Hence, only sophisticated problems concerning ClO, for example the mechanism of its dimerization, which yields different Cl_2O_2 isomers,[4] the rate constant of the HO_2 + ClO reaction[80] or highest rotational levels[81] are the subject of further studies. Most synthetic, kinetic, spectroscopic and photochemical aspects of the ClO_x ($x = 0-2$) family are presented in a recent comprehensive review.[1]

In the last decades less attention was focussed on the ClO_x ($x = 3, 4$) radicals, although the symmetric ClO_3 radical (C_{3v}) has a long history. ClO_3 was postulated as an intermediate in the formation of Cl_2O_6 from the reaction of Cl or OClO with O_3[50, 82–85] and in the decomposition of Cl_2O_6.[86] The structural, spectroscopic and chemical properties of ClO_3 and Cl_2O_6 have remained controversial over nearly 150 years.[47, 87–98] Finally, for Cl_2O_6, a X-ray crystallographic analysis of the low temperature solid has confirmed an ionic structure $ClO_2^+ClO_4^-$,[99, 100] while an IR gas phase and matrix isolation study have suggested a molecular structure of $O_2ClOClO_3$.[101–103] In the gas phase Cl_2O_6 decomposes rapidly into OClO and O_2 and is not in equilibrium with the anticipated ClO_3 radicals.[103] Countless attempts to study the formations and spectroscopic characteristics of ClO_3 have been failed. For example the thermal decay of Cl_2O_6 or Cl_2O_7 in the presence of fluorine,[104, 105] the reaction of ClO with singlet O_2,[106] the reaction between OClO and $O(^3P)$,[28, 68, 107–110] or the reaction of ClO_x ($x = 0-2$) with O_3.[111–114]

In 1994 ClO_3 radicals have been prepared for the first time by the low pressure pyrolysis of $ClOClO_3$ [Eq. (6)] followed by subsequent quenching of the products in low temperature matrices and are unambiguously characterized by IR and UV spectroscopy.[2]

$$ClOClO_3 \xrightarrow{\Delta} ClO + ClO_3 \quad (6)$$

ClO_3 shows a broad and structured UV/Vis spectrum beginning at about 750 nm with increasing intensity towards 300 nm. All four expected fundamentals for the $^2A_1$ ground state have been measured including the $^{35/37}Cl$ and $^{16/18}O$ isotopic species. Finally the formation of ClO_3 was supported by the excellent agreement between observed and calculated ab initio IR band positions and intensities.[2, 38–40, 115–119] In addition, time resolved UV spectra of pulse and γ-radiolysed or laser photolysed chlorate or perchloric acid solutions are assigned to ClO_3 or ClO_4 radicals, respectively.[120–122]

The existence of ClO_4 has also been controversial in the last 80 years as discussed;[85, 104, 105, 111, 113, 123–132] it was only in the late eighties of the last century that reinvestigations on the decay of Cl_2O_6[101, 103] lead to the trustworthy assumption that an intermediate ClO_4 radical is formed [Eq. (7.1)].

$$Cl_2O_6 \xrightarrow{\Delta} ClO_4 + ClO_2 \quad (7.1)$$

The first IR spectra of matrix isolated ClO_4 have been reported in 1996.[3] The ClO_4 radical was prepared by low pressure thermolysis of Cl_2O_6 with subsequent quenching of the products at low temperature in matrix. From the limited spectral data for ClO_4, C_{3v} symmetry was deduced. However, several new theoretical calculations on highest level predict C_{2v} or C_s symmetry.[39, 40, 119, 133, 134] Recently kinetic measure-

0947-6539/02/0824-5602 $ 20.00+.50/0 *Chem. Eur. J.* **2002**, *8*, No. 24

ments of the decay of Cl_2O_4 by reaction with chlorine atoms [Eq. (8)] lead to the assumption, that a stationary partial pressure of about 0.07 mbar ClO_4 may be possible in a steady state system.[135]

$$ClOClO_3 + Cl \rightarrow ClO_4 + Cl_2 \quad (8)$$

Another possible access to ClO_4 by γ-irradiation of solid perchlorates is promising, but the discussion and interpretation of the detected ESR signals have been controversial.[96, 97, 136–151]

Results and Discussion

The spectroscopic properties of short-lived radicals or molecules can be easily investigated if they are isolated in cryogenic matrices.[152–154] In a matrix-isolation experiment a high vacuum and the use of highly diluted precursor molecules during matrix deposition offer the appropriate conditions for the synthesis of short-lived radicals and molecules by low pressure flash thermolysis. In low pressure flash thermolysis an unimolecular bond fission of a fragile molecule A–B can be easily achieved, if the A–B bond energy is below 200 kJ mol^{-1}. If the bonds within both fragments A and B are stronger than 150 kJ mol^{-1}, little secondary bond cleavage of the A or B radicals should occur. These conditions are found to be true for several typical examples, that we studied in recent years. An early example is the fragmentation of peroxyacetyl nitrate (PAN)[155] [Eq. (9)] which leads to new spectroscopic data of the peroxyacetyl radical.

$$CH_3C(O)OONO_2 \rightarrow CH_3C(O)OO + NO_2 \quad (9)$$

Recent prominent experiments are the formation of CF_3O, CF_3OO and FCO_2 radicals by cleaving the thermally fragile precursors $CF_3OC(O)OOC(O)OCF_3$,[156] CF_3OONO_2[157, 158] and $FC(O)OOC(O)F$[159] with subsequent matrix isolation of the products according to Equations (10)–(12).

$$CF_3OC(O)OOC(O)OCF_3 \xrightarrow{\Delta} 2\,CF_3OCO_2 \rightarrow 2\,CF_3O + 2\,CO_2 \quad (10)$$

$$CF_3OONO_2 \xrightarrow{\Delta} CF_3OO + NO_2 \quad (11)$$

$$FC(O)OOC(O)F \xrightarrow{\Delta} 2\,FCO_2 \quad (12)$$

In order to generate ClO, ClO_3 or ClO_4 radicals in a similar manner, suitable precursor molecules containing a ClO, ClO_3 or ClO_4 fragment are needed. For this purpose we have investigated the low pressure flash thermolysis of $XOClO_3$ (X = H, F, Cl, ClO_2, ClO_3, NO_2) and $ClONO_2$ molecules. Other possible precursors $YOClO_2$ (Y = H, F, Cl, ClO_2, NO_2) are either unknown or extremely unstable and, therefore not available. In X-O-ClO_3 molecules, the terminal Cl–O bonds in ClO_3 are very strong and bond cleavage is possible only between XO–ClO_3 or X-$OClO_3$ [Eq. (13)–(15)].

$$ClO\text{-}ClO_3 \xrightarrow{\Delta} ClO + ClO_3 \quad (13)$$

$$O_2Cl\text{-}OClO_3 \xrightarrow{\Delta} OClO + ClO_4 \quad (14)$$

$$O_3ClO\text{-}ClO_3 \xrightarrow{\Delta} ClO_4 + ClO_3 \quad (15)$$

Which bond is cleaved, depends on the stability of the formed fragments. Therefore, in $ClOClO_3$ or $O_2ClOClO_3$ the stable fragment radicals ClO or ClO_2 are expected to be formed and the ClO_3 or ClO_4 radical should be the counterpart, respectively.

The thermal dissociation can be predicted from the molecular structures and bond energies. The structures of $XOClO_3$ molecules have been investigated by electron diffraction in the gas phase. In all cases the longest bond for XO-ClO_3 (X = H, F, Cl) amounts 164, 170, 171 pm, respectively[160] and the related bond energies are estimated to be 250, 181 and 150 kJ mol^{-1}, respectively.[161, 162] Therefore, the best precursor for the ClO_3 radical should be ClO-ClO_3.

Indeed, the best results have been achieved by the thermolysis of $ClOClO_3$ or $FOClO_3$. In regard to by-products we have used, $ClOClO_3$ for recording IR spectra and $FOClO_3$ for recording the UV spectra, because the UV absorption of the XO, XOO or $(XO)_2$ by-products for X = F are blue-shifted in comparison to the species with X = Cl and they interfere less with the UV absorptions of ClO_3. At higher temperatures, which are needed for the cleavage of HO-ClO_3 or O_3Cl-$OClO_3$, increased amounts of ClO_2 are formed.

Covalently bound Cl_2O_6 isomerizes into ionic $ClO_2^+ClO_4^-$ in the solid state below $-5\,^\circ C$;[101, 102] the related NO_2ClO_4 is even ionic ($NO_2^+ClO_4^-$) at room temperature.[163] As discussed above such X-$OClO_3$ (X = ClO_2, NO_2) molecules are promising precursors for the ClO_4 radical. The molecular structure of O_3Cl-$OClO_3$ with an O–Cl bond length of 172 pm indicates a weak bond[164, 165] and hence it may be a precursor for both ClO_3 and ClO_4 radicals. The estimated bond energies for O_2Cl–$OClO_3$, O_3Cl–$OClO_3$, and O_2N–$OClO_3$ are 100, 140 and 92 kJ mol^{-1}, respectively.[161, 162] Therefore the best precursor for ClO_4 radicals should be NO_2ClO_4. However, the vapour pressure of NO_2ClO_4 at room temperature is not sufficient for matrix isolation and at elevated temperatures solid NO_2ClO_4 decomposes. Another possible precursor for ClO_4 may be O_3ClO–$OClO_3$, because the isoelectronic FSO_2O-OSO_2F is well known and an excellent source for FSO_3 radicals.[166] However, all attempts for the synthesis of $O_3ClOOClO_3$ or the mixed peroxide FSO_2OOClO_3 have failed so far. The best precursor for ClO radicals is $ClONO_2$ due to its low ClO–NO_2 bond energy of 109 kJ mol^{-1}.[167]

Photoreactions in matrices are a powerful tool to create new species, which are not accessible by other reaction pathways. The cage effect is one of the most important features of matrix isolation. This effect is not available in the gas phase. The central question is, whether the photo fragments escape from the matrix cage and and if not, how do the fragments rearrange? If a fragment is small and symmetrical, for example a hydrogen atom ($^2S_{1/2}$), it may escape from the cage. In contrast, halogen ($^2P_{3/2}$) or oxygen ($^3P_{3/2}$) atoms are nonsymmetrical in their ground state. Hence, they should hardly escape but add again to a favoured side of the parent fragment; this results in an isomerization of the parent species. The size of the cage is the limiting factor of this photoinduced process.

Several photochemical isomerization reactions of chlorine oxides are well known: The monomer of chlorine dioxide OClO transforms into the chlorine superoxide ClOO on irradiation with light of wavelength $\leq$ 475 nm.[31] In this case

the O atom is the mobile agent, linking to the O atom of the parent fragment. An example for a mobilised Cl atom is the Y-shaped chloryl chloride, $ClClO_2$. It shows a typical cage effect: In the small cage of a neon matrix Cl_2 and O_2 are formed on irradiation at $\lambda \geq 495$ nm, while in argon matrix there is enough space for a rotational motion of the OClO fragment. At $\lambda \leq 610$ nm $ClClO_2$ isomerises into chlorine chlorite ClOClO, which undergoes a further transformation into dichlorine peroxide ClOOCl.[4] Johnsson et al. have shown that this is also true for $XClO_2$ with X = Br while for X = I even the argon cage is too small.[168]

For a deeper understanding of the photo isomerisation mechanism, we have reinvestigated the photolysis of ClO_x ($x = 1-4$) in oxygen matrices. The advantage of these experiments is that the mobile O atom will be caught mainly by the reactive oxygen matrix material forming ozone. A fragment is left behind, to which the O atom would have been added in the case of a non-reactive matrix.

Chlorine Monoxide

Many spectroscopic studies on gaseous ClO, which is a weak IR[1, 169, 170] and strong UV[1, 68–70] absorber, have been performed in the past. We want to report here on the influence of different matrix environments on the energetic states of ClO and on recent observations of its dimerization. In addition, the recorded spectra will be used as reference in the analysis of the spectra of ClO_3 and ClO_4 discussed below.

Low pressure flash pyrolysis of $ClONO_2$, highly diluted in a matrix gas with subsequent quenching of the products on a cold matrix support, leads to ClO, NO_2 and minor amounts of ClOClO according to the IR spectra. Hence, the thermolysis may proceed as follows [Eq. (16)–(19)].
primary:

$$ClONO_2 \xrightarrow{\Delta} ClO + NO_2 \quad (16)$$

secondary:

$$2\,ClO \rightarrow ClOClO \quad (17)$$

$$2\,ClO \xrightarrow{\Delta} Cl_2 + O_2 \quad (18)$$

or:

$$2\,ClO \rightarrow 2\,Cl + O_2 \quad (19)$$

The IR spectrum of ClO: The vibrational wavenumber of ^{35}ClO is found to show very little dependency on the environment (the respective ^{37}ClO band position is in all cases identical to the calculated value from the two-mass model). In Ne matrix (843.8 cm^{-1}) it is 0.5 cm^{-1} red-shifted in comparison to the gas-phase value of 844.20 cm^{-1}[171, 172] and in other matrix materials (Ar: 844.9; N_2: 848.2; Kr: 848.8; O_2: 849.4 cm^{-1}) blue-shifts are observed. This trend is unusual, because there are very often increased red-shifts of stretching modes of matrix isolated molecules with increasing polarisability of the matrix material.[173] Because the oxygen matrix behaves like an inert matrix material, there should be only a weak chemical interaction between ClO and oxygen. Concerning the interaction between ClO and O_2, interesting observations summarized in our previous ClO_3 paper[2] are now confirmed and extended by new and improved experiments. By UV photolysis of Ne matrix isolated ClO_3 radicals two new ^{35}ClO bands at 844.0 and at 839.5 cm^{-1} appear; the latter is tentatively assigned to a $ClO \cdot O_2$ complex. However, by comparing with the ^{35}ClO wavenumber in oxygen matrix (849.4 cm^{-1}) one would expect a significant blue shift for a $ClO \cdot O_2$ complex. Since the former band is only slightly blue-shifted (+0.2 cm^{-1}), this band is assigned to ClO radicals, isolated in a Ne matrix cage, which are little disturbed by an oxygen molecule. The latter band shows a red shift (−4.3 cm^{-1}) and is assigned to a $ClO \cdot O_2$ complex. For further details on this puzzle see section below on chlorine trioxide. There is another interesting feature in the IR spectra of ClO isolated in Ne matrices from the gas phase (without any O_2): A weak additional band at 838.5 cm^{-1} is always observed, which is close to the band of the $ClO \cdot O_2$ complex at 839.5 cm^{-1}. A possible interpretation is that this band is due to ClO in the $^2\Pi_{1/2}$ state. This assignment arises from the analysis of the UV spectrum of Ne matrix isolated ClO (see below) where a $A^2\Pi_{1/2} \leftarrow X^2\Pi_{1/2}$ subsystem is observed. This is only possible, if the $X^2\Pi_{1/2}$ state, which is higher in energy by 318 cm^{-1} than the $X^2\Pi_{3/2}$ ground state,[174] is still present after matrix deposition. Therefore we assume for the $X^2\Pi_{1/2}$ state of matrix isolated ClO a relaxation time of several hours. In the gas phase the vibrational wavenumber of the $X^2\Pi_{1/2}$ state is about 3.3 cm^{-1} lower than that of the $X^2\Pi_{3/2}$ state.[171, 172] In the Ne matrix IR spectra of ClO, produced by pyrolysis of $ClONO_2$ or $ClOClO_3$, a weak satellite 5.3 cm^{-1} below the absorption of ^{35}ClO in the $X^2\Pi_{3/2}$ state indicates the presence of a small fraction of ^{35}ClO in the $X^2\Pi_{1/2}$ state.

The UV spectrum of ClO: The UV spectrum of the pyrolysis products of $ClONO_2$, isolated in a neon matrix, is shown in Figure 1. From this spectrum, reference spectra of NO_2 and residual $ClONO_2$ have been subtracted, until a proper baseline for the final spectrum of ClO results. An identical UV spectrum can be obtained in a similar manner from the precursor $ClOClO_3$. The cross section scale in Figure 1 is adopted from the NO_2 gas phase values[137, 158] and the

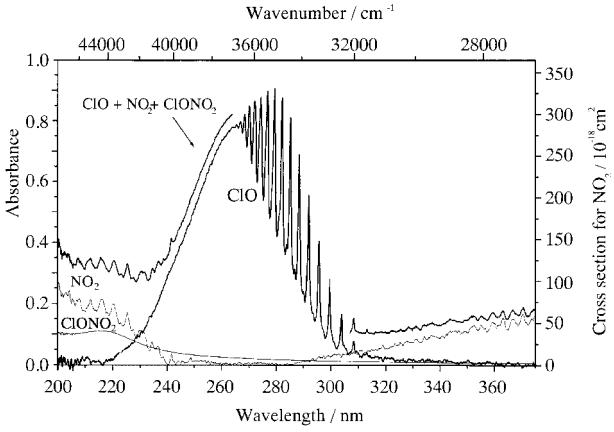

Figure 1. UV spectrum of ClO isolated in a neon matrix. Upper trace: raw spectrum of the thermolysis product of $ClONO_2$. Middle trace: reference spectrum of NO_2 and $ClONO_2$ (lower trace).

0947-6539/02/0824-5604 $ 20.00+.50/0 Chem. Eur. J. 2002, 8, No. 24

resulting absorption cross sections of ClO are listed in Table 1. Assuming that ClO and NO_2 are produced at a 1:1 molar ratio according to Equation (16) the cross sections for ClO are estimated to be too low. The difference in the cross section of matrix isolated ClO compared with the gas-phase values (Table 1) is attributed to side reactions during the thermolysis and quenching process [Eqs. (17)–(19)]. Due to the low concentration of ClOClO and other undetectable ClO dimers, these species should not contribute to the raw UV spectrum. At the absorbance maximum of Cl_2 near 330 nm no interference of the ClO band profile can be seen in Figure 1. Hence the main loss of ClO must occur in the heated nozzle with formation of chlorine atoms and dioxygen [Eq. (19)].

In the gas phase, the UV cross sections of the continuum is independent of temperature, while the structured part is extremely resolution and temperature dependent.[1, 69] Comparing our NO_2 based Ne matrix cross sections with literature gas-phase data at the beginning of the continuum at 260 nm, these values can be adjusted with a scaling factor of 1.88 (Table 1). Then the resulting values of the continuum are in excellent agreement with literature data,[62, 66, 69] whereas the values of Simon et al.[70] show a slower decrease at shorter wavelengths. In comparison to the structured part of the gas-phase spectrum, there are no hot band transitions and no rotational fine structures in the Ne matrix spectrum. Very surprising is the presence of the A $^2\Pi_{1/2} \leftarrow X^2\Pi_{1/2}$ subsystem, as already mentioned above. The scaled cross sections of the progression bands are in good agreement with literature values (see Table 1) up to the vibrational excited state (9,0). Due to interactions with the matrix phonon bands, the bands become broader and less intensive at higher excitations. Another reason for the band broadening is the transitions of the $A^2\Pi_{1/2} \leftarrow X^2\Pi_{1/2}$ subsystem, which interfere at higher excitations with the $A^2\Pi_{3/2} \leftarrow X^2\Pi_{3/2}$ system.

The progression of both subsystems has been analysed and the resulting spectroscopic data of the excited states are compared with the gas-phase data in Table 2. Both, the band origin and the vibrational wavenumber of ClO are only slightly affected by the matrix, while the anharmonicity is strongly increased. The latter effect is also seen in Table 1: The maxima of the progression bands are red-shifted at the beginning and blue-shifted at higher quantum numbers. This trend can be rationalized by increased repulsion of the ClO motions on the matrix with higher quantum numbers.

Table 2. Spectroscopic data [cm^{-1}] of $^{35}Cl^{16}O$ in the gas phase and isolated in a Ne matrix.

Ground state		Excited state	ν (0,0)	ω_e	$\chi_e\omega_e$
gas phase					
$X^2\Pi_{3/2}$	844.20[a]	$A^2\Pi_{3/2} \leftarrow X^2\Pi_{3/2}$	31 482[b]	520[b]	7.2[b]
$X^2\Pi_{1/2}$	840.92[a]	$A^2\Pi_{1/2} \leftarrow X^2\Pi_{1/2}$	31 685[b]		
Ne matrix[c]					
$X^2\Pi_{3/2}$	843.76	$A^2\Pi_{3/2} \leftarrow X^2\Pi_{3/2}$	31 408	526	8.9
$X^2\Pi_{1/2}$	838.5	$A^2\Pi_{1/2} \leftarrow X^2\Pi_{1/2}$	31 670	527	10.3

[a] Ref. [171, 172]. [b] Ref. [174]. [c] This work.

Table 1. Absorption cross sections of ClO ($A^2\Pi_{3/2} \leftarrow X^2\Pi_{3/2}$) isolated in a Ne matrix and in the gas phase.

	Ne matrix			Gas phase				
	λ[a]/(nm)	σ[b]/(10^{-20} cm^2)		λ/(nm)	σ/(10^{-20} cm^2)			
Transition		slit 0.3 nm			0.3 nm[c]	0.3 nm[d]	0.22 nm[e]	[f]
1,0	313.2 (312)	15.1	28.4	312.5			26	
2,0	308.4 (305.7)	30.5	57.3	307.9	39	58	47	
3,0	303.9 (301.6)	59.3	112	303.5	86	103	104	
4,0	299.7 (297.5)	103	194	299.3	163	171	104	
5,0	295.8 (293.8)	153	288	295.4	255	253	207	
6,0	292.0 (290.2)	205	385	292.0	338	330	382	
7,0	288.5 (287.0)	257	483	288.4	448	438	516	
8,0	285.3 (283.9)	296	556	285.2	542	530	627	
9,0	282.3 (281.1)	322	605	282.3	608	598	667	
10,0	279.4 (278.5)	332	624	279.8	655	645	688	
11,0	276.9 (276.1)	330	620	277.2	679	675	680	
12,0	274.5 (274.0)	325	611	275.1	681	671	634	
13,0	272.2 (272)	320	602					
14,0	270.2 (271)	314	590					
15,0	268.5 (269)	304	572					
16,0	266.9 (267)	295	555					
17,0	265.5 (266)	291	547					
continuum	260.0	270	508	260.0	504	509	512	530
	257.7	256	481	257.7	488	480	485	485
	255.0	235	442	255.0	454	440	452	450
	250.0	191	359	250.0	376	351	352	360
	245.0	145	273	245.0	294	274		270
	240.0	103	194	240.0	222			190
	235.0	68	128					
	230.0	42	79					
	225.0	28	53					
	220.0	16	30					

[a] Values in parenthesis belong to the $A^2\Pi_{1/2} \leftarrow X^2\Pi_{1/2}$ subsystem. [b] Second values scaled with 1.88, see text. [c] Ref. [70]. [d] Ref. [69]. [e] Ref. [66]. [f] Ref. [65].

Dimerization of ClO: As mentioned above, some dimerization of ClO is always observed during deposition of ClO in a matrix. Chainlike ClOClO is formed by head-to-tail interaction of two ClO and the resulting ClOClO shows a characteristic, strong IR band at 994.5 and 985.8 cm^{-1} ($^{35/37}ClO^{35}ClO$, $^{35/37}ClO^{37}ClO$, Ar matrix). This dimer has been observed already in very early matrix isolation experiments of ClO.[175–178] In later quantum chemical calculations it was pointed out, that three different isomers ClOOCl, $ClClO_2$ and ClOClO should exist with decreasing thermodynamic stability, respectively,[179–182] of these, $ClClO_2$ has the highest kinetic stability, which can be prepared by F/Cl exchange from $FClO_2$.[183, 184] Matrix-isolated $ClClO_2$ can be converted photolytically into the two other isomers.[4, 184] In the homogenous gas phase, ClOOCl is formed by

dimerization of ClO and characterized by microwave spectroscopy.[185] On the other hand for example on ice surfaces ClO dimerization leads to the isomer $ClClO_2$.[186] Hence, just which species of the three Cl_2O_2 isomers are formed, strongly depends on the reaction conditions.

Chlorine Dioxide

Since the first detailed IR matrix isolation study on OClO and its photolysis product ClOO,[187] many further spectroscopic investigations on both isomers in different matrices have been performed. IR absorption spectra of OClO and its isomer ClOO, isolated in inert matrices[5, 188] and in crystalline ice,[36, 37, 189] have been studied extensively. The UV spectra of ClOO[5, 188] and of OClO[5, 31] isolated in a Ne matrix have been measured and analysed. Recently, dispersed laser-induced fluorescence spectra of the $A^2A_2 \rightarrow X^2B_1$ transition of OClO in solid Ne have been recorded.[190] Mode specifity by photodissociation in a molecular beam[29] and site selectivity by laser photolysis of OClO in solid rare gases have been observed and the influence of different matrices on the conversion factors $\Delta A_{ClOO}/(-\Delta A_{OClO})$ were discussed.[31]

In all these studies appreciable amounts of OClO dimers are present in the matrices, which caused some problems in the interpretation of the results. In order to contribute to the understanding of the $(OClO)_2$ interference, we want to report here mainly on the $(OClO)_2$ dimer and in addition on the photochemistry of ClO_2 and $(OClO)_2$, isolated in an oxygen matrix.

The IR spectrum of the $(OClO)_2$ dimer: In the solid state, OClO forms weakly bound dimers as depicted of C_i symmetry with the following structural parameters.[13] These dimers partially survive sublimation at $-120\,^{\circ}C$ and can be trapped in

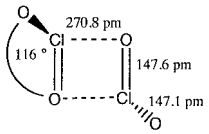

a matrix within a few milliseconds. We believe, that they maintain a similar structure. In this manner it has been possible to prepare matrices with a high fraction on OClO dimers. By heating the spray on nozzle in front of the matrix support and by using more highly diluted matrices, the contents of dimers are strongly reduced. Typical IR spectra for such an experiment are depicted in Figure 2.

The 12 vibrational motions of the OClO dimer are subdivided according to the irreducible representation [Eq. (20)].

$$\Gamma_{vib} = 6\,A_g\,(Ra, p) + 6\,A_u\,(IR) \qquad (20)$$

The two IR active ClO stretching modes and the OClO bending mode are observed in close proximity to the fundamentals of the monomer. All other fundamentals are expected to be observed in the far IR region and in the Raman spectrum. The band at 1107 cm^{-1} is obscured by the fundamental of the monomer and at 935 cm^{-1}, the 9:6:1 $^{35/37}Cl$ isotopic pattern is typical for a species, containing two equivalent chlorine atoms. The experimental IR data of $(OClO)_2$ are collected in Table 3.

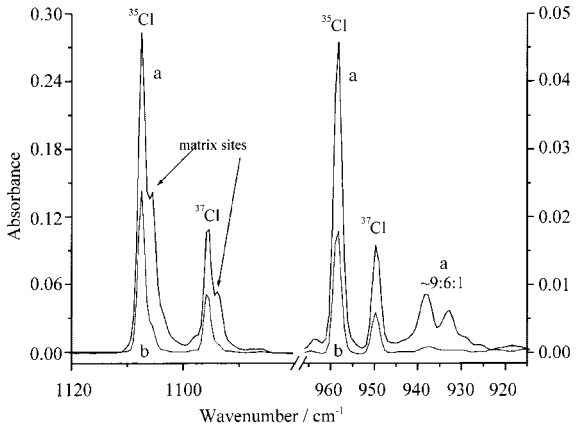

Figure 2. IR spectrum of OClO isolated in a neon matrix. a) OClO with a high content of $(ClO_2)_2$ dimers. b) Monomeric OClO.

Table 3. Experimental vibrational wavenumbers [cm^{-1}] for $(ClO_2)_2$.

Mode	Crystalline 77 K and 193 K[a]		Neon matrix[b]
ν_{as} ClO_2	1062 vbr.	1063 vbr	1107 1096
ν_s ClO_2	908	913	931, 927, 925/≈9:6:1
δ_s ClO_2	471	465	464 br, 451 br/≈9:6
ν Cl_2O_2	187	177	175 br

[a] Ref. [13]. [b] Ref. [5] and this work.

The UV spectrum of the $(OClO)_2$ dimer: Figure 3 presents the UV/Vis spectra of the same samples, which were used for recording the IR spectra in Figure 2. Traces a and b possess the known progression pattern of OClO, but in trace b an underlying continuum absorption is present. The weighted

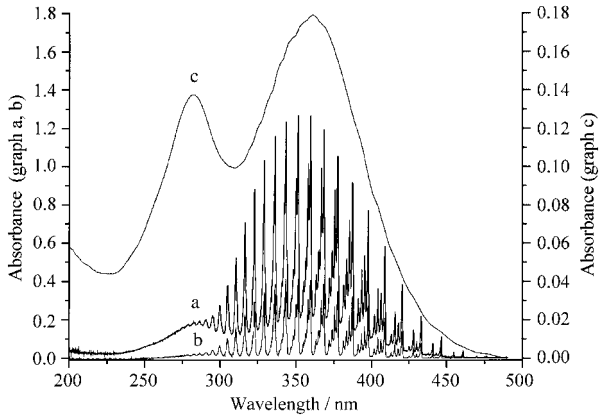

Figure 3. UV/Vis spectrum of OClO isolated in a neon matrix. a) OClO with a high content on $(ClO_2)_2$ dimers. b) Monomer OClO. c) Difference spectrum a) – b); $(ClO_2)_2$ in expanded scale.

difference b – a which yields the smoothed trace c represents the unstructured UV/Vis spectrum of the $(OClO)_2$ dimer. A continuum absorption of OClO is mentioned by Wahner et al.[23] but its origin and intensity are not well understood. Liu et al.[190] report recently, that their OClO continuum might be due to an absorption of the 1^2A_1 state above its predissociative barrier, but we suppose, that there is a continuum due to dimeric chlorine dioxide.

Photochemistry of matrix isolated OClO: In order to understand the different conversion factors $\Delta A_{ClOO}/(-\Delta A_{OClO})$ in

0947-6539/02/0824-5606 $ 20.00+.50/0 Chem. Eur. J. 2002, 8, No. 24

dependence of the matrix material and the excitation energy,[31] we have studied the OClO photolysis also in an oxygen matrix. There is no obvious interaction of OClO and its isomer ClOO with oxygen, because with respect to the wavenumbers of the OClO and ClOO fundamentals, the oxygen matrix behaves like an argon matrix. However, the photochemistry of OClO in solid oxygen is quite different from that in solid rare gases. After primary photodissociation of OClO into ClO+O within the oxygen matrix cage, the surrounding O_2 molecules compete with ClO in the reaction with the oxygen atom. According to the resulting IR spectra the main product is O_3. In addition some ClOO and the by-product ClO is clearly seen. The ratio of the product band absorbances, O_3/ClOO, increases with increasing energy of the photolysis light. This means, that the oxygen atom escapes more efficiently from the matrix cage with increasing excess energy of the photolysis light source. This loss of oxygen atoms must be taken in account also in solid rare gases. It becomes more pronounced in the order Ne < Ar < Kr. The $(OClO)_2$ dimer behaves similarly. In rare gas matrices it is converted mainly to $ClOClO_3$ and a small fraction of $ClOClO_2$.[5] But in an oxygen matrix, the yield of $ClOClO_2$ is much higher, because of effective oxygen atom scavenge by the surrounding oxygen molecules. UV photolysis ($\lambda > 230$ nm) of the O_2 matrix for a longer period of time causes a decrease of bands due to $ClOClO_3$, $ClOClO_2$ and ClO and increase of the bands of ClOO. Hence the final end products Cl+O_2 of all chlorine oxides are formed.

Chlorine Trioxide

In the course of our preliminary study of matrix-isolated ClO_3 radicals, IR and UV/Vis spectra have been measured and analysed to only some extent.[2] In particular the reported UV spectrum is strongly perturbed by absorptions due to the by-products ClO and OClO and to the precursor $ClOClO_3$. We want to present here further spectroscopic data and their detailed analysis, in order to characterize this short lived radical more comprehensively.

The IR spectrum of ClO_3: Low pressure flash pyrolysis of $ClOClO_3$, highly diluted in a matrix gas, in front of the matrix support with subsequent quenching of the products in matrix leads to ClO, ClO_3, some ClO_2 and minor amounts of ClOClO, Cl_2O_6 and Cl_2O_3. The formation of these products is assumed to proceed as follows [Eqs. (21)–(26)].

primary:

$$ClOClO_3 \xrightarrow{\Delta} ClO + ClO_3 \quad (21)$$

secondary:

$$ClO + ClO_3 \rightarrow 2\,OClO \quad (22)$$

$$ClO_3 \xrightarrow{\Delta} ClO_2 + O \quad (23)$$

$$2\,ClO_3 \rightarrow O_2ClOClO_3 \quad (24)$$

$$2\,ClO \rightarrow ClOClO \quad (25)$$

$$ClO + ClO_2 \rightarrow ClOClO_2 \quad (26)$$

Figure 4 shows a typical IR spectrum of matrix isolated ClO, and ClO_3 as products after subtracting the bands of ClO_2 and residual $ClOClO_3$ (the ranges are indicated by arrows). All band positions and their relative integrated intensities of ClO_3

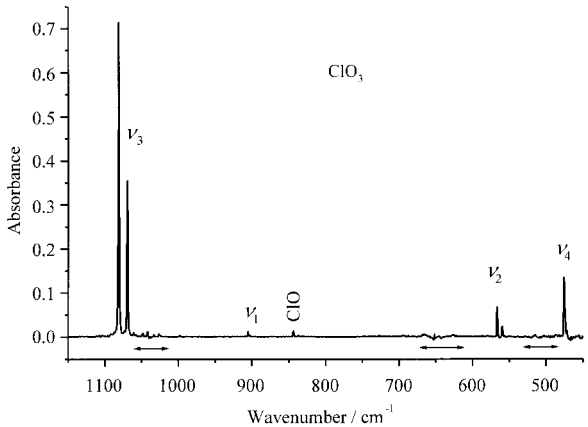

Figure 4. IR spectrum of ClO_3 and ClO isolated in a neon matrix. The radicals are produced by low pressure thermolysis of $ClOClO_3$. Bands of residual $ClOClO_3$ and of some by-products are subtracted in the regions indicated by arrows.

as well as of the $Cl^{18}O_3$ isotopomer are collected in Table 4. Also included are the overtones and combinations, which have not been reported before.[2] The band positions are shifted to lower wavenumbers from Ne to Ar or O_2 matrix, as expected for matrices with higher polarizability, and O_2 behaving similar to an Ar matrix. Hence ClO_3 does not react with O_2 to form the peroxy radical O_3ClOO as does the isoelectronic CF_3 radical;[157, 191, 192] both radicals have 25 valence electrons. The identity of all observed ClO_3 bands is confirmed by their constant relative band intensities in

Table 4. Vibrational wavenumbers [cm^{-1}] of isotopic ClO_3 species exhibiting C_{3v} symmetry isolated in Ne, Ar and O_2 matrix.

Ne matrix[a]					Ar matrix[a]		O_2 matrix[a]		Assignment[b]
$^{35}Cl^{16}O_3$	I[c]	$^{37}Cl^{16}O_3$	$^{35}Cl^{18}O_3$	$^{37}Cl^{18}O_3$	$^{35}Cl^{16}O_3$	$^{37}Cl^{16}O_3$	$^{35}Cl^{16}O_3$	$^{37}Cl^{16}O_3$	
2155.31	3.5	2131.77	2087.0	2062.4	2137.0	2113.5	2139.8	2116.2	$2\nu_3$, A_1
1970.4	13	1956.3	1892.7	1877.7	1955.3	1941.2	1958.3	1944.1	$\nu_1 + \nu_3$, E
1641.9	0.7	1623.0	1590.7	1571.3	1640.4	1620.8	1630.8	1612.0	$\nu_2 + \nu_3$, E
1081.27	100	1069.44	1047.06	1034.69	1072.2	1060.3	1074.0	1062.2	ν_3, e $\nu_{as}(ClO_3)$
905.04	3	902.59	860.23	857.45	899.5	897.0	900.4	897.8	ν_1, a_1 $\nu_s(ClO_3)$
566.63	11	559.44	549.63	542.48	562.7	555.6	563.0	555.9	ν_2, a_1 $\delta_s(ClO_3)$
475.76	20	474.09	452.14	450.66	473.3	471.8	474.1	472.6	ν_4, e $\delta_{as}(ClO_3)$

[a] Most intensive matrix site, average of several measurements. [b] According to C_{3v} symmetry. [c] Integrated relative infrared intensities, $I(\nu_3) = 100$.

  0947-6539/02/0824-5607 $ 20.00+.50/0

experiments using different precursors and thermolysis temperatures, as well as by photolysis of the matrix using light of wavelength >530 nm, which causes a decrease in intensity for all ClO_3 bands. The presence of ClO_3 radicals with C_{3v} symmetry is evident from the following facts: i) the IR bands display an isotopic pattern (3:1), in accordance with a species, containing one chlorine atom; ii) in experiments with $Cl_2{}^{18}O_4$ containing about 70% ^{18}O four isotopomers are detected, consistent with a species containing three equivalent oxygen atoms; iii) four IR active fundamentals are observed for ClO_3 (C_{3v}) in accordance with the irreducible representation [Eq. (27)]:

$$\Gamma_{vib} = 2\,a_1\ (IR, Ra\ p) + 2\,e\ (IR, Ra\ dp) \qquad (27)$$

iv) for the mixed isotopomers $Cl^{16}O_2{}^{18}O$ and $Cl^{16}O^{18}O_2$ of C_s symmetry, the e modes are split into a′ and a″ components, as shown in Figure 5 (Table 5); and v) good agreement of observed IR data and predicted from quantum chemical calculations (see Table 6).

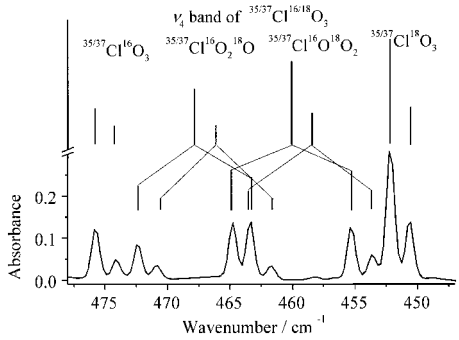

Figure 5. The ν_4 bands of an isotopic mixture of ClO_3. The components are compared with a simulated spectrum.

All these observations leave no doubt regarding the presence of ClO_3 and confirm the assignment of the vibrational bands. In Figure 5 the ν_4 bands of the four isotopomers $Cl^{16}O_3$, $Cl^{16}O_2{}^{18}O$, $Cl^{16}O^{18}O_2$ and $Cl^{18}O_3$ were simulated using the molar ratio of 1:1.6:2.3:3.0, respectively. For the mixed species $Cl^{16}O_2{}^{18}O$ and $Cl^{16}O^{18}O_2$ the lower and higher wavenumber components are of a′ symmetry, respectively, because the in plane atom in both cases is involved mostly in the a′ mode. Also the overtones and combination modes of *E* symmetry show the same isotopic pattern as do the e-type fundamentals. Predicted IR spectra and geometric parameters of high level ab initio and DFT calculations are given in Table 6. The results agree quite well with the observed IR spectrum of ClO_3 isolated in a Ne matrix, which resembles closely the gas phase situation of the free radicals. The smallest deviations from experiment are seen for calculations, using UB3LYP and B3LYP methods.

Table 5. Vibrational wavenumbers [cm^{-1}][a] of mixed isotopomers of ClO_3 isolated in Ne matrix.

$^{35}Cl^{16}O_2{}^{18}O$	$^{37}Cl^{16}O_2{}^{18}O$	$^{35}Cl^{16}O^{18}O_2$	$^{37}Cl^{16}O^{18}O_2$	assignment C_{3v}	C_s
2148.4	2124.7	2113.9	2089.8	$2\nu_3$ E	a″
2124.7	2101.0	2131.8	2107.4		a′
1956.2	1941.9	1904.3	1889.2	$\nu_1+\nu_3$ E	a″
1932.6	1917.6	1932.2	1917.6		a′
1635.9	1616.1	1597.2	1577.9	$\nu_2+\nu_3$ E	a″
1616.1	1597.2	1620.6	1601.7		a′
1081.3	1069.4	1047.1	1034.9	ν_3 e	a″
1060.6	1048.3	1071.3	1059.5		a′
888.3	885.5	873.5	870.7	ν_1 a_1	a′
561.1	554.1	555.5	548.4	ν_2 a_1	a′
472.4	470.9	464.8	463.4	ν_4 e	a″
463.4	461.7	455.3	453.7		a′

[a] Most intensive matrix site.

Evaluation of the molecular structure of ClO_3: The experimental bond angle is calculated from the observed vibrational data by using the sekular Equation [Eq. (28)][193] for the symmetry class e in the point group C_{3v}.

$$|\boldsymbol{G}^*\boldsymbol{F}| = |\boldsymbol{E}^*\lambda| \qquad (28)$$

For $\boldsymbol{G}$ matrix: geometric parameters, masses; $\boldsymbol{F}$ matrix: force constants; $\boldsymbol{E}$: unit matrix; λ: Eigenvalues. Under the assumption that the F matrix for each symmetry class is equal for the different isotopomers[193] and λ is proportional to ω^2 (harmonic wavenumber) the following Equation (29) is valid.

$$\frac{\prod_i \omega_i^2}{\prod_i \omega'^2_i} = \left|\frac{G}{G'}\right| \qquad (29)$$

This Equation is a special form of the Redlich – Teller product rule.[193] By using the matrix elements $\boldsymbol{G}_{ij}$[194] and calculating for different angles the six possible quotients of the determinants $\boldsymbol{G}$ and $\boldsymbol{G}'$ for the four isotopomers $^{35}Cl^{16}O_3$, $^{37}Cl^{16}O_3$, $^{35}Cl^{18}O_3$, and $^{37}Cl^{18}O_3$ it is shown, that only the quotients in the symmetry class e are dependent of the OClO bond angle. Figure 6 shows two of the six plots $\det|\boldsymbol{G}/\boldsymbol{G}'|$ against the OClO bond angle (two with a positive slope and four with a negative slope) in the symmetry class e. The values for the quotients of the square products of the observed wavenumbers obtained from the isotopic pairs $^{35}Cl^{16}O_3/^{37}Cl^{16}O_3$ and $^{35}Cl^{16}O_3/^{37}Cl^{18}O_3$ lead to the bond angles 110.3 and 130.6°, respectively. The large discrepancy between both results is

Table 6. Calculated vibrational wavenumbers [cm^{-1}], band intensities (km mol^{-1}, in italic), bond length [pm] and bond angle [°] of $^{35}Cl^{16}O_3$.

Method	MP2[a]	RMP2[b]	B3LYP[c]	UB3LYP[d]	B3LYP[e]	SVWN[f]	exptl[g]
mode e		1180 (*77*)	1050 (*110*)	1081	1080	1095	1081 (*100*)
a_1		987 (*2*)	903 (*4*)	924	923	921	905 (*3*)
a_1		581 (*21*)	551 (*21*)	564	564	548	567 (*11*)
e		479 (*16*)	464 (*12*)	472	471	450	476 (*20*)
r (Cl–O)	148.1	149.2	149.2	145.2	145.4	146.1	148.5 ± 2
∢ (OClO)	114.6	113.8	113.8	114.2	114.1	114.1	113.8 ± 1

[a] Ref. [116]. [b] Ref. [117]. [c] /cc-pVQ(5)Z, Ref. [40]. [d] Ref. [39]. [e] Ref. [118]. [f] Ref. [38]. [g] This work, relative integrated band intensities in italic.

0947-6539/02/0824-5608 $ 20.00+.50/0 *Chem. Eur. J.* **2002**, *8*, No. 24

due to the anharmonic nature of the experimental wavenumbers. They can be corrected by introduction of the anharmonic constants δ_i according to Equation (30).

$$\frac{\prod_i \omega_i^2}{\prod_i \omega_i'^2} = \left(\frac{\nu_3 \cdot (1+\delta_3)}{\nu_3' \cdot (1+\delta_3'')}\right)^2 \cdot \left(\frac{\nu_4 \cdot (1+\delta_4)}{\nu_4' \cdot (1+\delta_4')}\right)^2 = \frac{\prod_i \nu_{\text{corr.}}^2}{\prod_i \nu_{\text{corr.}}'^2} = \left|\frac{G}{G'}\right| \tag{30}$$

With the approximation: $\nu_{\text{obs}} \cdot (1+\delta) - \nu_{\text{obs}}' \cdot (1+\delta') = \Delta\nu_{\text{obs}} \cdot (1+\delta'') = \Delta\omega$,[195] Equation (30) can be rearranged to Equation (31).

$$\frac{\prod_i \omega_i^2}{\prod_i \omega_i'^2} = \left(\frac{\nu_3}{\nu_3 - \Delta\nu_3 \cdot (1+\delta_3''')}\right)^2 \cdot \left(\frac{\nu_4}{\nu_4 - \Delta\nu_4 \cdot (1+\delta_4''')}\right)^2 = \frac{\prod_i \nu_{\text{corr.}}^2}{\prod_i \nu_{\text{corr.}}'^2} = \left|\frac{G}{G'}\right| \tag{31}$$

As seen in Figure 6 each ratio of determinants can be described as an approximate linear function of the bond angle α [Eq. (32)].

$$\left|\frac{G}{G'}\right| = \boldsymbol{m} \cdot \alpha + \boldsymbol{b} \leftrightarrow \left(\frac{\prod_i \nu_{\text{corr.}}^2}{\prod_i \nu_{\text{corr.}}'^2} - \boldsymbol{b}\right) \cdot m^{-1} = \alpha \tag{32}$$

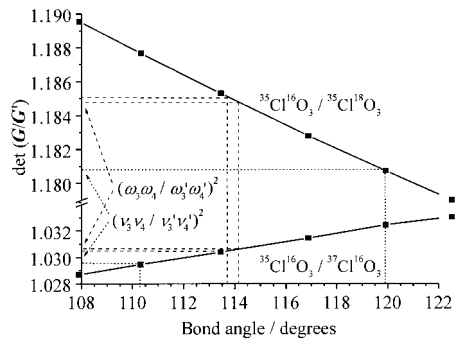

Figure 6. Plots of $|\boldsymbol{G}|$ matrix element ratios in the representation *e* for different ClO_3 isotopomers versus the OClO bond angle. Pointed lines indicate the observed $(\nu_3 \cdot \nu_4/\nu_3' \cdot \nu_4')^2$ values. After a proper anharmonicity correction (see text) the dashed lines lead to the α_e bond angle (113.8°) of ClO_3.

By varying δ_3''' and δ_4''', in principle a corrected bond angle can be obtained, although there are several possible solutions. Taking into account that the potential of a deformation mode in general is less anharmonic than a stretching mode (due to the non-dissociative character of the deformation mode) one can assume a δ_4'''/δ_3''' ratio in the range of 0 to 0.25. With this assumption matching of the bond angle for two $|\boldsymbol{G}/\boldsymbol{G'}|$ slopes can be obtained by varying δ_3''' (dashed lines in Figure 6). By using all eight combinations of the six quotients (2 positive slope × 4 negative slope) an average bond angle of 113.8 ± 0.7° is obtained. This bond angle should resemble the α_e value for ClO_3 in the gas phase within ±1°, because it has been shown for the similar OClO radical that the bond angle determined from Ne matrix vibrational data[5] is identical within the estimated error limit of ±0.2° to the α_e gas phase value.[196]

With the bond angle of ClO_3 obtained as discussed above, calculations of the general valence force field using the NCA program[197] are performed. As input data all wavenumbers of the four fundamentals of eight isotopomers (Tables 4 and 5) are used after the required anharmonic corrections are performed according to Becher.[195] All data are iterated simultaneously until minimum least square deviation between observed and calculated vibrational data are obtained. The result is presented in Table 7. Due to the large number of independent vibrational isotopic input data (>10) all six inner-force constants are overestimated and should be reliable. This is a rare case and comparison with ab initio values would be desirable. However, to our knowledge such data are not available from the literature at present. Most striking is the unusual large interaction force constant $f_{\alpha\alpha}$ which causes a large potential energy distribution (PED) for ν_2 and ν_4. In other molecules $f_{\alpha\alpha}$ may be much smaller. Hence in the ClO_3 radical the OClO bending causes a strong electron flow to the neighbouring bonds. Use of the stretching force constant f_r offers an estimate of the ClO bond length. For this purpose ClO force constants of different species containing ClO bonds (Table 8) are plotted against their respective bond length and fitted with an exponential function (Figure 7).

Table 7. Force constants (10^2 N m^{-1}, normalized on 100 pm bond length) and potential energy distribution (PED) of ClO_3.

Force constants		PED			
	NCA	ν_3	ν_1	ν_2	ν_4
f_r	6.780	1.00	0.96		
f_{rr}	0.156				
$f'_{r\alpha}$	0.050				
$f_{r\alpha}$	0.228				
f_α	2.472			0.52	1.74
$f_{\alpha\alpha}$	1.103			0.46	−0.78

Table 8. Structural parameters (pm, °, 10^2 N m^{-1}) for different species containing ClO bonds.

	Cl_2O[a]	HOCl[b]	ClO[c]	FClO[d]	OClO[e]	$ClClO_2$[f]	$FClO_2$[g]	$FClO_3$[h]
r_e (ClO)	169.59	168.91	156.96	148.4	146.98	143.68	141.99	139.7
∢ OClO	–		–		117.4	114.63	115.03	115.8
f (ClO)	2.959	3.79	4.71	7.04	7.03	8.52	9.36	10.13

[a] Ref. [198–200]. [b] Ref. [201, 202]. [c] Ref. [81, 203]. [d] Ref. [203]. [e] Ref. [19]. [f] Ref. [204]. [g] Ref. [205, 206]. [h] Ref. [203, 207].

Assuming a 90% confidence level, the ClO bond length is estimated to be 148.5 ± 2 pm. The estimated structural parameters of ClO_3 from vibrational data, termed "experimentally" are compared in Table 6 with calculated parameters. Our "experimental" structure is within the error limits in accordance with most theoretical predictions. A future accurate structural determination either by microwave or/and high resolution IR spectroscopy is needed, to decide, which prediction is optimal.

The UV/Vis spectrum of ClO_3: In order to record UV spectra of ClO_3 with less interference from by-products as reported in

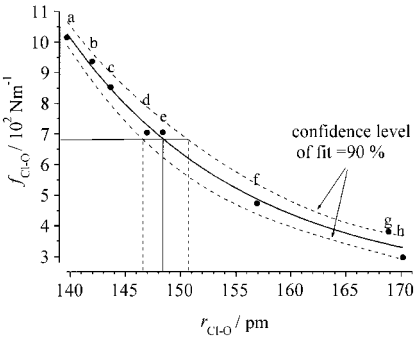

Figure 7. Correlation of ClO force constants versus ClO bond lenghts for different ClO species. With the ClO force constants of ClO_3 6.78 (see text) a ClO bond length of 148.5 pm is estimated. Under consideration of a 90% confidence level of the exponential fit the error is estimated to be ± 2 pm. a) $FClO_3$, b) $FClO_2$, c) $ClClO_2$, d) ClO_2, e) FClO, f) ClO, g) ClOH, h) ClOCl.

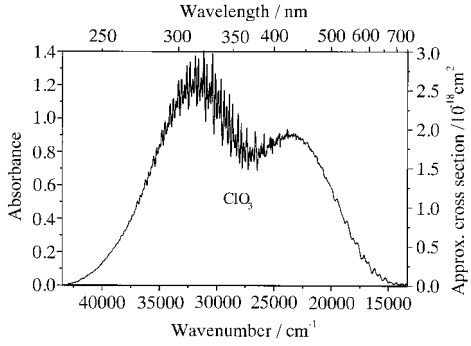

Figure 8. UV/Vis spectrum of ClO_3 isolated in a neon matrix. The radical is produced by low pressure thermolysis of $FOClO_3$. Bands of by-products are subtracted by using reference spectra (see text).

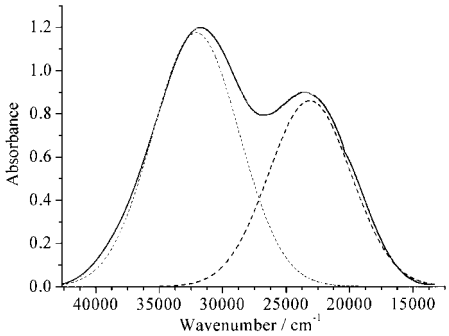

Figure 9. Smoothed UV/Vis spectrum of ClO_3 presented in Figure 8. Dashed lines are simulated Gaussian profiles of the bands.

our previous note,[2] we mainly use $FOClO_3$ as source for ClO_3 in this study. After low pressure flash thermolysis of $FOClO_3$ with subsequent isolation of the products in a Ne matrix, the IR spectrum shows $FOClO_3$ and ClO_3 along with the by-products FO, FOO, FOOF and ClO_2. Hence it can be assumed that the reaction proceeds as follows [Eqs. (33) – (37)].
primary:

$$FOClO_3 \xrightarrow{\Delta} FO + ClO_3 \quad (33)$$

secondary:

$$FO + FO \rightarrow FOOF \quad (34)$$

$$FOOF \xrightarrow{\Delta} FOO + F \quad (35)$$

$$FO + ClO_3 \rightarrow FOO + OClO \quad (36)$$

$$ClO_3 \xrightarrow{\Delta} OClO + O \quad (37)$$

A crude UV/Vis spectrum averaged from the five "best" flash thermolysis experiments has been recorded, as well as the reference UV spectra of OClO and $FOClO_3$. The unstructured spectra of FOO, and FOOF, taken from literature,[208, 209] are added to the reference spectrum of $FOClO_3$ according to the estimated portions in the thermolysis experiments. This leads to a synthetic reference spectrum in the 200 – 270 nm range. Applying both reference spectra for computational spectra subtraction of the by-products, to the raw spectrum, the spectrum presented in Figure 8 is obtained. Smoothing of the absorption profile and fitting both bands with Gauss functions leads to the spectrum depicted in Figure 9.

The high energy band is found at $\nu_{max} = 32100\ cm^{-1}$ (311.5 nm), a half width of $6800\ cm^{-1}$, an onset (0 – 0 transition) at $\approx 20000\ cm^{-1}$, and the low energy band at $\nu_{max} = 23150\ cm^{-1}$ (432.0 nm), half width $6400\ cm^{-1}$, onset at $\approx 13300\ cm^{-1}$. The band intensity ratio is 1:0.7. These results are in good agreement with a recent photoelectron study of the ClO_3^- anion[25] and the theoretically predicted electronic transitions of ClO_3.[210] In the photoelectron spectroscopy study of ClO_3^- with a 157 nm laser excitation three electronic states (X^2A_1, A^2A_1, B^2E) have been probed. The above-mentioned maxima of the electronic transition in the UV/Vis spectrum of ClO_3 can be correlated with the energy gaps between the adiabatic value of the ground state (X^2A_1) and the vertical detachment energies of the excited states. For the $A^2A_1 \leftarrow X^2A_1$ and $B^2E \leftarrow X^2A_1$ transition, this gap amounts to 1.5 ± 0.2 eV ($12100\ cm^{-1}$) and 2.85 ± 0.2 eV ($23000\ cm^{-1}$), respectively. The first excited state has a transition moment equal to zero[210] and is not observed experimentally. The second transition is in excellent agreement with the observed UV absorption. In a recent high level ab initio study of ClO_3,[210] using several different methods the vertical excitation energies into the A^2A_2, B^2E, and C^2E states are predicted to be in the range 1.25 – 1.49 eV ($\approx 11000\ cm^{-1}$), 2.55 – 2.90 eV ($\approx 22000\ cm^{-1}$) and 3.55 – 3.93 eV ($\approx 30200\ cm^{-1}$) with a relative transition moment for the last two transitions of about 1.2:1, respectively. Both calculated band maxima are on average a little too low and the band intensities are reversed, in comparison to the observed UV spectrum.

As demonstrated in the preceding chapters the UV spectra of ClO and OClO, isolated in Ne matrix, are in good agreement with their respective gas phase spectra. They are blue-shifted by only a few tenth of a nm; some minor effects caused by the rotational fine structure and hot bands in the gas-phase spectra are quenched in the matrix. Hence it can be assumed that the UV spectrum of ClO_3 depicted in Figure 8 corresponds very well to the yet unknown gas phase spectrum. The cross section scale placed on the right axis in Figure 8 is deduced from photolysis experiments. Photolysis with light $\lambda > 530$ nm causes a decrease of the ClO_3 absorption and a

  0947-6539/02/0824-5610 $ 20.00+.50/0 *Chem. Eur. J.* **2002**, *8*, No. 24

simultaneous increase of ClO absorption. With help of the generally accepted gas phase cross section of ClO ($\sigma_{max} = 5.2 \times 10^{-18}$ cm^2 at $\lambda_{max} = 260$ nm[211]) the cross section of ClO_3 $\sigma = 3.0\ (\pm 0.5) \times 10^{-18}$ cm^2 at the strongest progression band (11,0,0) at $\lambda = 321.15$ nm are adjusted.

The high-energy UV band, which is shown in Figure 10 on an expanded scale, exhibits a pronounced vibrational fine structure. The most intense peaks in this fine structure form the main progression and are separated by about 800 cm^{-1}. Each peak in this progression is accompanied by two satellites

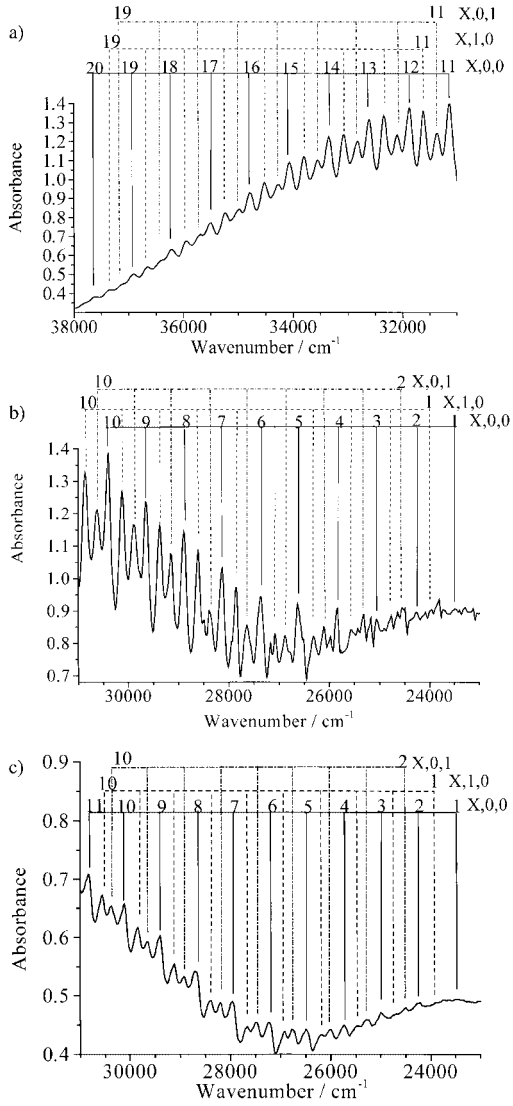

Figure 10. a) and b) Structured part of the UV/Vis spectrum of ClO_3 in expanded scale from Figure 8. c) Part b) for $Cl^{18}O_3$.

due to two additional vibrations in the excited C^2E state. Due to the antibonding nature of this excited state[210] all fundamentals should be lower than in the ground state (1081, 905, 567, 476 cm^{-1}). According to the selection rules, excitation of all fundamentals in the $C^2E \leftarrow X^2A_1$ transition is allowed.[212] A shifted asymmetric stretching mode (from $\approx$1080 to 800 cm^{-1}) seems to be the origin of the main progression, because its normal coordinate correlates well with the dissociation path into OClO+O,[210] and the relative isotopic vibrational shifts of $\Delta\nu(Cl^{16/18}O_3)/\nu(Cl^{16}O_3)$ which are equal in the ground and excited state. The first high energy satellite on each progression bands could be either a $\approx$250 or a $\approx$1050 cm^{-1} vibration depending whether it "sits" on the quantum number n or $(n-1)$ of the progression, respectively. Due to the choice of the asymmetric stretching vibration in the main progression and the antibonding nature of the excited state, we assume the first satellite "sits" on the quantum number n (blue-shifted by 250 cm^{-1}) and can be correlated with the symmetric deformation mode in the ground state (567 cm^{-1}). The second high energy satellite (blue-shifted by 500 cm^{-1}) can be correlated with the 905 cm^{-1} symmetrical stretching mode in the ground state.

As seen in Figure 10b, c the origin of the progression somewhere below 24000 cm^{-1} is uncertain. To determine the origin of the high energy UV band, the spectrum of $Cl^{18}O_3$ is measured (Figure 10c). The isotopic shifts between the bands of $Cl^{16}O_3$ and $Cl^{18}O_3$ are proportional to the quantum numbers and should be nearly zero at the origin of the transition. By fitting the linear difference of equivalent bands of $Cl^{16}O_3$ and $Cl^{18}O_3$ against arbitrary quantum numbers, the (0,0,0) transition is finally located at about 22700 cm^{-1}. With the true quantum numbers available, the whole progression spectra of both isotopomers are simulated with the second order approximation of Herzberg[213] [Eq. (38)].

$$\nu_{obs} = \nu_{00} + \sum_i \omega_i^0 \nu_i + \sum_i \sum_{k \geq i} \chi_{ik}^0 \nu_i \nu_k;\ \omega_i^0 = \omega_i + \chi_{ii} + 0.5 \sum_{i \neq k} \chi_{ik};\ \chi_{ik}^0 = \chi_{ik} \quad (38)$$

with ω_i^0 = harmonic wavenumber and χ_{ik}^0 = anharmonic constants. The observed wavenumbers are taken directly from the band maxima or they are examined from their second derivative spectra. For the simulation of the $Cl^{16}O_3$ data, the three harmonic wavenumbers and five anharmonicity constants were iterated simultaneously until the sum of deviations reached a minimum. Subsequently the anharmonicity constants are kept nearly constant for the simulation of the $Cl^{18}O_3$ data. The results of the simulation are presented in Tables 9 and 10. In general the deviation between observed and calculated band position in Table 9 are in the order of the uncertainty limits of the measured band positions. Hence the resulting parameters presented in Table 10 appear to be reliable. The anticipated much lower vibrations in the excited C^2E state and their assignments in comparison to the ground state are supported by their equivalent isotopic effects.

There is additional structure in the spectrum which may be due to matrix site splitting, a further vibration or the splitting of the e modes. Definitive conclusions, however, are not possible, because residual incompensations as a result of the spectra subtraction which causes some artefacts. The analysis of the fine structure of the low energy band does not lead to reasonable results, due to the overlapping of bands. It can be assumed that there is a main progression with several satellites with a band separation by 900 to 1000 cm^{-1}.

A critical evaluation of the literature data for other claims for the UV/Vis spectrum of ClO_3[96, 97, 120, 121, 140] leads to the conclusion that in all cases something else was observed, but not ClO_3. In a recent study on laser photolysis of peroxydisulfate solutions containing chlorate, a very broad unsym-

Table 9. Assignment for the progressions of Ne matrix isolated ClO_3 in the $C^2E \leftarrow X^2A_1$ transition.

Assignment			$Cl^{16}O_3$		$Cl^{18}O_3$		assignment			$Cl^{16}O_3$		$Cl^{18}O_3$	
			observed	diff.[a]	observed	diff.[a]				observed	diff.[a]	observed	diff.[a]
ν_3	ν_1	ν_2	x [cm^{-1}]				ν_1	ν_2	ν_3	x [cm^{-1}]			
0	0	0	22696		22696								
1	0	0	23482	−6	23441	−18	12	0	0	31883	2	31536	−6
1	0	1			23724	0	12	0	1	32098	−8	31776	10
1	1	0	23964	−16			12	1	0	32347	0	31974	−6
2	0	0	24269	−6	24207	−11	13	0	0	32616	1	32253	5
2	0	1	24545	2	24486	7	13	0	1	32825	−11	32483	14
2	1	0	24764	−1	24663	−17	13	1	0	33085	6	32680	−3
3	0	0	25063	6	24970	−2	14	0	0	33350	5		
3	0	1	25320	−1	25233	3	14	0	10	33551	−10		
3	1	0	25562	18	25430	−1	14	1	0	33807	1		
4	0	0	25840	5	25720	−1	15	0	0	34066	−3		
4	0	1	26103	9	25991	16	15	0	1	34275	−7		
4	1	0	26319	−1	26164	−14	15	1	0	34524	−4		
5	0	0	26635	28	26465	−1	16	0	0	34995	−2		
5	0	1	26881	19	26720	4	16	0	1	35236	−9		
5	1	0	27089	−1	26914	−6	16	1	0	35236	−9		
6	0	0	27367	−8	27205	0	17	0	0	35499	−5		
6	0	1	27640	14	27463	11	17	0	1	35707	−1		
6	1	0	27847	−8	27657	0	17	1	0	35958	0		
7	0	0	28129	−9	27946	6	18	0	0	36231	17		
7	0	1	28393	8	28188	5	18	0	10	36410	−4		
7	1	0	28612	−4	28381	−9	18	1	0	36670	4		
8	0	0	28898	2	28674	4	19	0	0	36910	−10		
8	0	1	29138	−1	28910	1	19	0	1	37120	5		
8	1	0	29369	−3	29112	–	19	1	0	37369	0		
9	0	0	29656	6	29394	−1	20	0	0	37643	23		
9	0	1	29881	−7	29643	12	20	0	1	37814	3		
9	1	0	30125	3	29841	1	20	1	0	38073	6		
10	0	0	30400	2	30111	−5	21	0	0	38314	−2		
10	0	1	30623	−9	30358	11	21	1	1	38513	−11		
10	1	0	31864	−5	30553	−5	21	1	0	38760	0		
11	0	0	31138	−4	30821	−10	22	0	0	38986	−21		
11	0	1	31373	2	31065	6				$\Sigma \lvert x \rvert = 235$[b]		$\Sigma \lvert x \rvert = 139$[c]	
11	1	0	31626	16	31269	−2							

[a] Observed − calculated = difference. [b] Quantum number 6 to 19 included. [c] Quantum number 6 to 13 included.

Table 10. Wavenumbers [cm^{-1}] and anharmonic constants of the normal modes of $Cl^{16}O_3/Cl^{18}O_3$ in the excited C^2E state.

Wavenumber[a]	Assignment	Anharmonic constant					
794 (1081) 766 (1047)	ω_1^0 e ν_{as}	χ_{11}	−2.4				
498 (905) 470 (860)	ω_2^0 a_1 ν_s	χ_{12}	−2.4	χ_{22}	−3.7		
280 (567) 272 (550)	ω_3^0 a_1 δ_s	χ_{13}	≈ -4.3 ≈ -3.7	χ_{23}	0	χ_{33}	−3.4

[a] In parenthesis ground state values, second values belong to $Cl^{18}O_3$.

metrical band with a maximum at about 330 nm and a flat band at about 450 nm has been reported.[122] The shape of this spectrum resembles in principle that of the ClO_3 spectrum in Figure 8, so that the following reaction sequence may have occured [Eq. (39)].

$$S_2O_8^{2-} + 2\,ClO_3^- \xrightarrow{h\nu} 2\,SO_4^- + 2\,ClO_3^- \xrightarrow{10-90\,\mu s} 2\,SO_4^{2-} + 2\,ClO_3 \quad (39)$$

In a similar way, the UV/Vis spectrum of the isoelectronic SO_3^- radical anion has been measured.[214] In comparison to the UV/Vis spectrum of ClO_3 the spectrum is structureless and blue-shifted by about 50 nm with a cross section of 4.0×10^{-18} cm^2 at 260 nm and a low energy band at 360 nm of much lower intensity, than the respective band of ClO_3.

The photochemistry of ClO_3: Photolysis of ClO_3 isolated in a Ne matrix with a tungsten halogen lamp in combination with a cut-off filter $\lambda > 455$ nm leads to ClO (^{35}ClO 844.0 and 839.5 cm^{-1}) and O_2 (1549.1 cm^{-1}) while ClO_3, isolated in a O_2 matrix, leads mainly to O_3 (1035.5, 702.4 cm^{-1}) and OClO (1104.7, 942.1, 453.4 cm^{-1}) after the same irradiation. In the former case the bands of ClO and O_2 are slightly shifted in comparison to the direct matrix isolated species (^{35}ClO 843.8; O_2 1554 cm^{-1}). The primary step after excitation into the B^2E state is dissociation [Eq. (40)].

$$ClO_3 \xrightarrow{h\nu} OClO + O \quad (40)$$

In Ne matrix, reaction of the oxygen atom with OClO occurs in the matrix cage according to Equation (41).

$$OClO + O \rightarrow ClO + O_2 \quad (41)$$

In O_2 matrix the O atom reacts with one of the surrounding O_2 molecules and O_3 is formed. Two different $ClO \cdot O_2$ complexes are formed in a Ne matrix as indicated by the two IR bands at 844.0 and 839.5 cm^{-1}. In addition a new UV

0947-6539/02/0824-5612 $ 20.00+.50/0 *Chem. Eur. J.* **2002**, *8*, No. 24

absorption on the short wavelength wing of the ClO band appears (Figure 11).

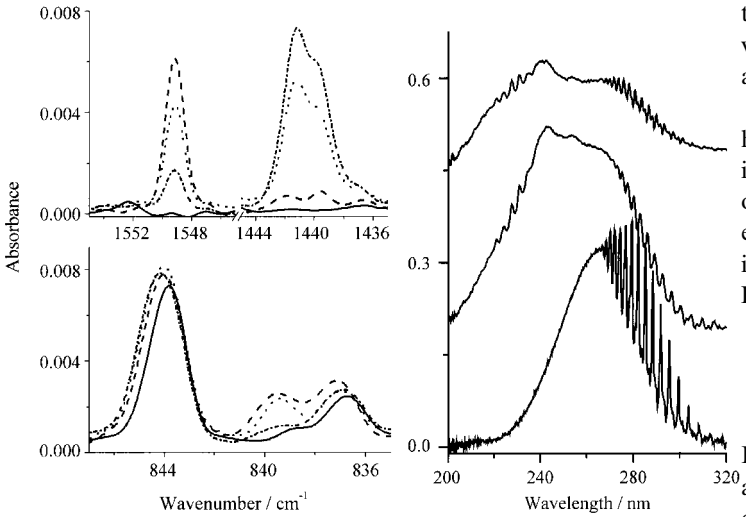

Figure 11. IR and UV spectra of the low pressure thermolysis products of $ClOClO_3$ isolated in a neon matrix. (——): IR spectrum of monomeric ^{35}ClO (843.8 cm^{-1}) ^{37}ClO (836.8 cm^{-1}) in the $^2\Pi_{3/2}$ state and ^{35}ClO (838.5cm^{-1}) in the $^2\Pi_{1/2}$ state. Lower trace; right: UV spectrum of ClO after subtraction of the bands of all by-products (compare with Figure 1). (----): IR-spectrum after visible light photolysis ($\lambda > 455$ nm) of about 80% of the matrix isolated ClO_3 yielding $^{35}ClO \cdot O_2$ (844.0 cm^{-1}) $^{37}ClO \cdot O_2$ (837.0 cm^{-1}) in the $^2\Pi_{3/2}$ state and $^{35}ClO \cdot O_2$ (839.5 cm^{-1}) in the $^2\Pi_{1/2}$ state. At 1549.1 cm^{-1} the O_2 stretching band of $ClO \cdot O_2$ in the $^2\Pi_{1/2}$ state is shown. Middle trace, right: difference UV spectrum (photolysis minus thermolysis) of $ClO \cdot O_2$. In contrast to ClO obtained by thermolysis (lower trace) the higher populated $^2\Pi_{1/2}$ state is clearly shown. · · · and •–•–: IR spectra after 255 nm photolysis for 10 and 30 min. Mainly the complex $ClO \cdot O_2$ ($^2\Pi_{1/2}$) disappeared (839.5 cm^{-1}) and at 1440 cm^{-1} ClOO appeared. Upper trace: difference UV spectrum (photolysis 455 nm minus photolysis 255 nm) indicating mainly the loss of $ClO \cdot O_2$ ($^2\Pi_{1/2}$).

Further photolysis of the Ne matrix at 255 nm (high-pressure Hg lamp + cut-off filter) causes a decrease of the IR bands at 839.5 and 1549.1 cm^{-1}, a small increase of the band at 844.0 cm^{-1}, appearance of a new band at 1441 cm^{-1} (ClOO) as well as disappearance of the new UV band. The change of the UV spectrum is displayed in Figure 11. These findings can be interpreted as follows: On photolysis of ClO_3 in Ne matrix, a complex of the composition $ClO \cdot O_2$ in analogy to the $FO \cdot O_2$ complex[215] is formed, which is characterized by two UV bands (see Figure 11) and an IR band at 839.5 cm^{-1}. Additionally, a second $ClO{-}O_2$ species is formed, which is assigned to a ClO radical situated next to an oxygen molecule in the same Ne matrix cage showing a weaker interaction. The former complex (839.5 cm^{-1}) is more photosensitive at 255 nm, than the latter ClO species (844.0 cm^{-1}) and is depleted into several channels: i) It is converted into the weak $ClO \cdot O_2$ complex (844.0 cm^{-1}, maybe the isomer $OCl \cdot O_2$) with an IR inactive O_2 molecule; ii) an oxygen atom left the matrix cage and some ClOO (1441 cm^{-1}) is formed and iii) it dissociates into O_2+Cl+O. In the difference UV spectrum before and after photolysis at 255 nm, mainly a peroxy radical band at $\approx$260 nm with a vibrational progression of $\approx$670 cm^{-1} and, in the ClO region, the $^2\Pi_{1/2}$ subsystem are clearly seen. Hence, we interpret the new UV and IR (839.5, 1549.1 cm^{-1}) absorber as a $ClO \cdot O_2$ complex with ClO in the excited $^2\Pi_{1/2}$ state.

There is another interesting observation: Visible light photolysis of Ne matrix isolated ClO_3 causes an intensity increase of the weak bands of Cl_2O_6, which are formed during the deposition process. Presumably a small fraction of $(ClO_3)_2$ van der Waals dimers are activated in this manner and asymmetric bond linking of $(ClO_3)_2$ to $O_2ClOClO_3$ occurs.

The experimentally observed threshold for slow (5% in one hour) photodissociation of ClO_3 is at 610 nm. With more intense light sources, the threshold may be observable at the onset of the absorption band at $\approx$750 nm. Interestingly the energy of the onset ($\approx$160 kJ mol^{-1}) is within the uncertainty, identical to the first Cl–O bond energy of ClO_3 calculated by Francisco[118] and Janoschek.[40]

Chlorine Tetroxide

In our preliminary study of matrix isolated ClO_4 radicals IR and UV/Vis spectra are recorded and analysed in some detail.[3] Based on the five observed IR bands C_{3v} symmetry for the radical was assumed. However, several recent theoretical studies disagree with this conclusion and C_{2v} symmetry is predicted.[38–40, 133, 134] We want to report here on an extended spectroscopic study of this elusive radical, in order to establish an experimental basis for final conclusions.

The IR spectrum of ClO_4: Dichlorine hexoxide, Cl_2O_6, is the best precursor for the synthesis of ClO_4 radicals and is used throughout in this study. Low pressure flash pyrolysis of Cl_2O_6, highly diluted in a matrix gas in front of the matrix support with subsequent quenching of the products at low temperatures, leads to ClO_2, ClO_4, ClO_3 and minor amounts of $HClO_4$. The formation of these products is assumed to proceed as follows [Eqs. (7.2, 42–45)].
primary:

$$O_2Cl\text{-}OClO_3 \xrightarrow{\Delta} ClO_2 + ClO_4 \quad \text{major path} \qquad (7.2)$$

$$O_2ClO\text{-}ClO_3 \xrightarrow{\Delta} 2\,ClO_3 \quad \text{minor path} \qquad (42)$$

secondary:

$$ClO_4 \xrightarrow{\Delta} ClO_2 + O_2 \qquad (43)$$

$$ClO_4 + H_2O \rightarrow HClO_4 + OH \qquad (44)$$

Neon matrix reference spectra of all by-products and Cl_2O_6 are recorded for use of computational spectra subtraction. After "treatment" of the ten best raw neon matrix spectra of the Cl_2O_6 pyrolysis products, with these reference spectra the resulting spectra are averaged and smoothed. The final spectrum is presented in Figure 12.

It shows three further weak IR absorptions in addition to the five known bands of ClO_4.[3] Since the relative intensities of the new bands are the same in all experiments and since they decrease uniformly after photolysis of the matrix (tungsten-halogen lamp, cut off filter $\lambda > 495$ nm), all bands should belong to ClO_4. Further support for the identity of the new bands and their assignment come from experiments with isotopically enriched $Cl_2{}^{18}O_6$. In the spectral regions of the

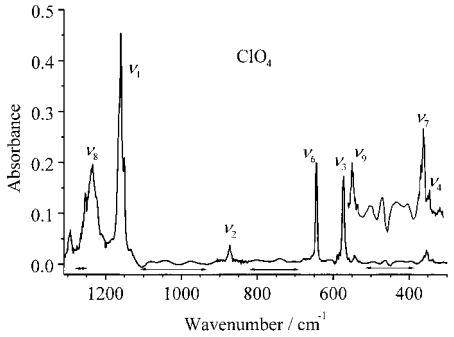

Figure 12. IR spectrum of ClO_4 isolated in a neon matrix. Bands of residual Cl_2O_6 and of by-products (Cl_2O_4, ClO_2, $HClO_4$) are subtracted and the regions are indicated by arrows.

fundamentals the eight observed IR bands, including their $Cl^{18}O_4$ counterparts, are presented in Figure 13 in expanded scale. All vibrational band positions and relative band intensities are gathered in Table 11.

With the increased number of IR active fundamentals, the ClO_4 radical must exhibit a lower symmetry than C_{3v} as previously assumed.[3] Depending on the possible symmetries C_{2v} or C_s the nine vibrational motions of ClO_4 are divided into the irreducible representations [Eqs. (45) and (46)].

$$C_{2v}: \Gamma_{vib} = 4\,a_1\ (IR, Ra\ p) + a_2\ (-) + 2\,b_1\ (IR, Ra\ dp) + 2\,b_2\ (IR, Ra\ dp) \quad (45)$$

with 8 IR active fundamentals or

$$C_s: \Gamma_{vib} = 6\,a'\ (IR, Ra\ p) + 3\,a''\ (IR, Ra\ dp) \quad (46)$$

with nine IR active fundamentals. With the experimental data alone, one can not distinguish unambiguously between C_{2v} and C_s symmetry, because the activated a_2 mode in C_s symmetry can be very weak. To achieve a decision between C_{2v} and C_s, the vibrational data in Table 11 are compared with the theoretical predicted data in Tables 12 and 13. According to most theoretical calculations, the ClO_4 radical should possess C_{2v} symmetry, with two short and two long ClO bonds forming bond angles of about 114 and 95°, respectively (see Table 12). The observed and calculated wavenumbers in Table 12 and their isotopic shifts in Table 13 are in agreement with the observed vibrational data and hence ClO_4 should exhibit C_{2v} symmetry at the minimum of its potential hypersurface.

However, calculated and experimental IR band intensities give in general a much poorer fit than to band positions. The intensity of the ν_8 band is overestimated by 80% and ν_2 by about 250%. The calculated intensities of the bands ν_3, ν_4, ν_6, ν_7 deviate over a greater range but in average they fit well to the experimental intensities. The greatest deviation exhibits the ν_9 band, which has only 10–20% of the calculated intensity.

A particular feature of the ClO_4 IR matrix spectrum is the broadness of the absorption bands with half widths of up to 20 cm^{-1}. At higher resolution (0.13 cm^{-1}) a fine structure of the band profile appears, as shown for example in Figure 13d at the ν_6 band. At least six components can be seen and we assume that they are caused by matrix site splittings, which are unusually pronounced in ClO_4 (normally the half width of IR matrix bands are 0.1–1 cm^{-1}). The reason for this feature may be the Jahn–Teller effect in ClO_4 resulting in a distortion from T_d symmetry and a shallow potential minimum.[133, 134] In this situation, the ClO_4 radicals "feel" the different matrix cages more than an ordinary molecule and the superposition of all spectra for all different matrix sites (here >6) leads to broad bands. Furthermore, the theoretical calculations point out, that a second stable structure of ClO_4 with C_s symmetry lies only ≈4–5 kJ mol^{-1} above the C_{2v} minimum.[133, 134] The ClO_4 radicals are produced at about 500 K and with regard to the Boltzmann distribution a noticeable amount of ClO_4 with the C_s structure should be present in the heated spray on

Table 11. Vibrational wavenumbers [cm^{-1}][a] of ClO_4 isolated in Ne, Ar and O_2 matrix.

Ne matrix[b]			Ar matrix			Assignment		O_2 Matrix					
$^{35}Cl^{16}O_4$	$^{37}Cl^{16}O_4$[b]	I[c]	$^{35}Cl^{18}O_4$	$^{35}Cl^{16}O_4$	$^{37}Cl^{16}O_4$[b]	/description of mode[d] C_{2v} symmetry		$^{35}Cl^{16}O_4$ site A	$^{35}Cl^{16}O_4$ site B	$^{37}Cl^{16}O_4$ site A	$^{37}Cl^{16}O_4$ site B	I[c]	Approx. description of mode
		≈2280 br				$2\nu_8$	A_1						
≈2243	≈2220	≈1				$2\nu_1$	A_1						
≈1811		≈1	≈1727			$\nu_8+\nu_6$	A_2						
≈1760 br		≈1	≈1690 br		≈1750	$\nu_8+\nu_3$	B_2[e]						
≈1695 br		≈3	≈1620 br		≈1685	$\nu_1+\nu_3$	A_1						
≈1480 br		≈3	≈1410 br		≈1475	$\nu_1+\nu_7$	A_1	1525.4	1528.8			50	ν (O–O)
≈1457 br		≈1	≈1390 br		≈1450	$\nu_2+\nu_6$	B_1						
≈1412 br		≈2	≈1345 br		≈1405	$\nu_2+\nu_3$	A_1						
1292.5	1287.7	7	1252		≈1285	ν_1 C_s ClO_4[f]							
1233.6	1221.6	100	1196.4	1227	1217	ν_8 $\nu_{as}(Cl^sO_2)$	b_2	1252.1	1244.7	1238	1234	100	ν_{as} (ClO_3)
1207 br		≈3				$\nu_6+\nu_3$	B_1	1229.4	1196.6	1216.6	1185		
1160.8	1150.4	100	1118.2	1154	1144	ν_1 $\nu_s(Cl^sO_2)$	a_1						
1132 br		≈3				$2\nu_3$	A_1	1012.7	1002.3	1010.5	1000	24	ν_s (ClO_3)
873.0		4	831.3	≈872		ν_2 $\nu_s(Cl^lO_2)$	a_1						
644.3	642.1	16	608.4	641	639	ν_6 $\nu_{as}(Cl^lO_2)$	b_1	687.8br	≈681.5	667.0	660.5	58	ν (Cl–O)
573.0	569.9	16	545.5	570	564	ν_3 δ (Cl^sO_2)	a_1						
544.3	540.9	2	518.8			ν_9 $\omega/\rho(ClO_2)$	b_2	593.6	589.4		585	15	δ_{as} (ClO_3)
354.0	350.5	3	345.6			ν_7 $\delta(Cl^lO_2)$	a_1	573.5	576.3	569			
337.2	(334.8)	1	321.2			ν_4 ω/ρ (ClO_2)	b_1						

[a] Peak position at the main matrix site. [b] Shoulders or peaks at the $^{35}ClO_4$ isotopomer band, localized from the second derivative spectrum. [c] Relative infrared intensities integrated over all matrix sites and isotopomers. [d] Cl^sO_2 short Cl–O bonds, Cl^lO_2 long Cl–O bonds. [e] Also possible $\nu_8+\nu_9\,A_1$, $\nu_1+\nu_6\,B_1$. [f] Or $2\nu_6$ of C_{2v} ClO_4 in Fermi resonance with ν_8, see text.

0947-6539/02/0824-5614 $ 20.00+.50/0 *Chem. Eur. J.* **2002**, *8*, No. 24

Table 12. Calculated vibrational wavenumbers [cm^{-1}], intensities ($km\,mol^{-1}$, in italic) bond lengths [pm] and bond angles [°] of $^{35}Cl^{16}O_4$ (C_{2v}).

Mode	B3LYP/ cc-pVQZ[a]		UB3LYP[b]		TZ2P++ B3P86[c]		TZ2P++ B3LYP[c]		cc-pVDZ UHF-CCSD(T)[d]		exptl[e]	
ν_8 b_2	1233	(*183*)	1257	(*182*)	1229	(190)	1263	(*186*)	1257	(*189*)	1234	(100)
ν_1 a_1	1137	(*150*)	1160	(*150*)	1132	(*157*)	1161	(*151*)	1161	(*157*)	1161	(100)
ν_2 a_1	879	(*17*)	904	(*18*)	868	(*17*)	878	(*18*)	850	(*12*)	873	(4)
ν_6 b_1	623	(*25*)	648	(*22*)	615	(20)	612	(18)	609	(*12*)	644	(16)
ν_3 a_1	561	(*27*)	572	(*27*)	550	(26)	562	(24)	547	(*34*)	573	(16)
ν_9 b_2	541	(*17*)	550	(*15*)	532	(15)	555	(15)	531	(*26*)	544	(2)
ν_7 b_1	400	(*3*)	413	(*2*)	397	(*2*)	366	(*6*)	450	(*4*)	354	(3)
ν_4 a_1	379	(*2*)	385	(*1.7*)	374	(2)	383	(2)	391	(*2*)	337	(1)
ν_5 a_2	367	(*0*)	375	(*0*)	355	(*0*)	362	(*0*)	347	(*0*)	–	
r ($Cl-O^s$)	141.4		141.44		142.4		143.3		146.6			
r ($Cl-O^l$)	148.8		148.62		150.2		151.6		155.2			
∢ (O^sClO^s)	114.0		113.97		114.2		114.3		114.3			
∢ (O^lClO^l)	94.6		94.75		93.6		93.5		91.4			

[a] Ref. [40]. [b] Ref. [39]. [c] Ref. [133], B3LYP is scaled with 1.07. [d] Ref. [134], scaled with 1.07. [e] This work, relative integrated band in tensities in italic.

nozzle and should be quenched without relaxation in the matrix. The calculated vibrational wavenumbers for ClO_4 in C_{2v} and C_s symmetry are similar and may overlap each other. However, the most intensive and short-waved band is predicted to occur in the range of 1300 or 1260 cm^{-1} for $Cl^{16}O_4$ or $Cl^{18}O_4$, respectively.[133] In Figure 13a such an additional band (≈5–7% of ν_8) appears in this region, so that an assignment of this band to ClO_4 in the C_s form can be

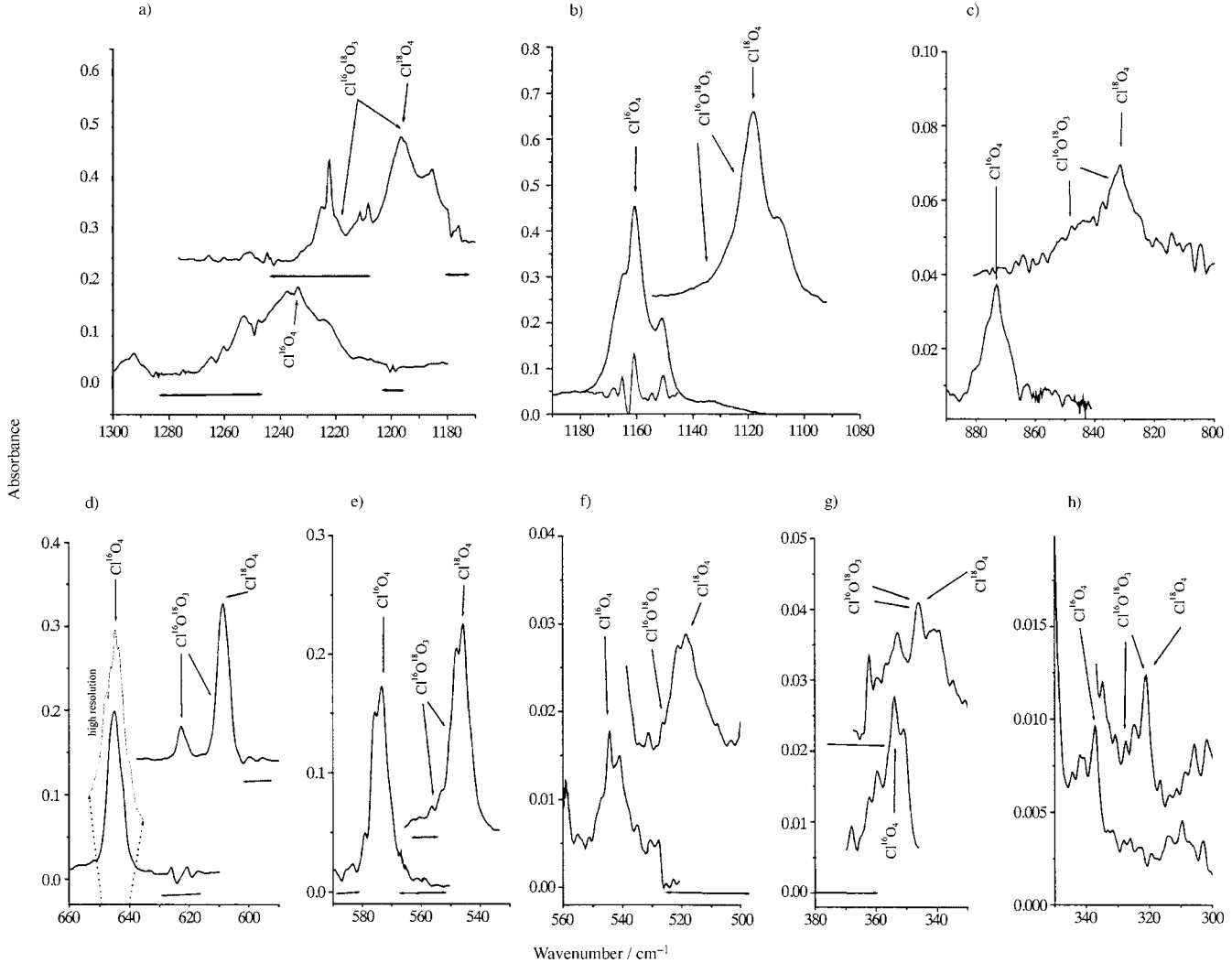

Figure 13. IR band regions of $Cl^{16}O_4$, $Cl^{18}O_4$ and $Cl^{16}O^{18}O_3$ in expanded scale. Arrows indicate calculated band positions (see text). Horizontal arrows indicate by-products subtraction regions

  0947-6539/02/0824-5615 $ 20.00+.50/0

Table 13. Calculated and experimental vibrational isotopic shifts (cm^{-1}) of ClO_4.

mode	Exptl wave-number	$\Delta\nu$ $^{35/37}Cl^{16}O_4$ calcd[a]	exptl[b]	calcd[c]	$\Delta\nu$ $^{35}Cl^{16/18}O_4$ calcd[d]	calcd[d]	exptl[b]
ν_8 b_2	1234	14.8	12	41.3	40	38	37
ν_1 a_1	1161	11.6	10.2	43.7	41	40	43
ν_2 a_1	873	1.8	–	48.5	47	44	42
ν_6 b_1	644	0.1	–	36.4	35	33	36
ν_3 a_1	573	3.1	3.1	26.6	25	26	28
ν_9 b_2	544	3.3	3.7	24.6	24	24	26
ν_7 b_1	354	6.3	3.5	8.7	8	7	8.4
ν_4 a_1	337	0.4	($\approx$2)	21.3	21	20	16

[a] This work, B3LYP/6-311G (d,p). [b] Shoulders or peaks at the $^{35}ClO_4$ isotopomer band, localized from the second derivative spectrum. [c] Ref. [39], UB3LYP. [d] Ref. [133], TZ2P^{++}B3P86 and TZ2P^{++}B3LYP.

taken into account. Hence, an additional reason for the broadness of the bands is seen in an easy distortion of the C_{2v} structure in direction towards of the C_s structure.

For evaluation of the $^{35/37}ClO_4$ isotopic shifts (see Table 13) the second derivative spectra are used as shown for the ν_1 band in Figure 13b (this band is undisturbed by precursor and by-product bands). Three groups of two bands separated by 10.2 cm^{-1} ($\Delta\nu$ $^{35/37}ClO_4$) are clearly seen.

The IR spectrum of ^{18}O isotopically labelled ClO_4, which contains about 15% $Cl^{16}O^{18}O_3$, possesses another interesting feature. For an estimate of the band positions of the $Cl^{16}O^{18}O_3$ isotopomer, we calculated the wavenumbers of the $Cl^{16}O_4$, $Cl^{18}O_4$ (C_{2v}),and $Cl^{16}O^{18}O_3$ (C_s, with ^{16}O located at the short or long bond) fundamentals at the B3LYP/6-311G(p,d) level of DFT theory.[216] The results for the scaled wavenumbers of $Cl^{16}O^{18}O_3$ are gathered in Tables 14 and the band positions are

Table 14. Scaled calculated vibrational wavenumbers [cm^{-1}] of the $Cl^{16}O^{18}O_3$ in C_s symmetry based on the calculated and experimental vibrational wavenumbers for $Cl^{16}O_4$ and $Cl^{18}O_4$ in C_{2v} symmetry.

mode	$Cl^{16}O_4$, C_{2v} exptl	calcd[a]	$Cl^{18}O_4$, C_{2v} exptl	calcd[a]	factor[b]		$Cl^{16}O^{18}O_3$ C_s short[c] scaled[d]		$Cl^{16}O^{18}O_3$ C_s long[c] scaled[d]
ν_8 b_2	1234	1149	1196	1112	1.075	a′	1219	a″	1195
ν_1 a_1	1161	1055	1118	1017	1.100	a′	1134	a′	1122
ν_2 a_1	873	798	831	755	1.097	a′	835	a′	846
ν_6 b_1	644	543	608	512	1.187	a″	611	a′	622
ν_3 a_1	573	521	546	497	1.099	a′	557	a′	550
ν_9 b_2	544	504	519	481	1.079	a′	526	a″	526
ν_7 b_1	354	313	346	306	1.131	a″	347	a′	348
ν_4 a_1	337	358	321	338	0.945	a′	321	a′	327

[a] This work B3LYP/6-311G (d,p). [b] Scaling factor: exptl/calcd averaged value. [c] ^{16}O placed on the short or long bond. [d] This work B3LYP scaled with the factor from [b].

indicated by arrows in Figure 13. All band profiles of $Cl^{16}O_4$ and $Cl^{18}O_4$ should be the same, but they are distorted for $Cl^{18}O_4$ in all cases (see Figure 13). With the overlap of $Cl^{16}O^{18}O_3$ bands one can rationalize the changes in the $Cl^{18}O_4$ band profiles. Only for ν_6, one component of $Cl^{16}O^{18}O_3$ is clearly separated from $Cl^{18}O_4$. The appearance of this component is a further evidence for the two different ClO bonds in ClO_4.

In contrast to the other chlorine oxide radicals, ClO_4 interacts strongly with oxygen. The typical broad feature of the IR spectrum of matrix isolated ClO_4 vanishes completely, when oxygen is used as a matrix material. At 1525 cm^{-1} a strong OO stretching band is seen which is comparable to the analogous band of FOO, isolated in a oxygen matrix (1496 cm^{-1}).[217] Four additional groups with sharp IR bands appear near 1250, 1010, 690 and 590 cm^{-1}, which are all split into two components (site A and B) as in the OO stretching band. There is an interesting site selectivity by photolysis. After irradiation of the O_2 matrix with light of wavelength >395 cm^{-1} the intensity of site B bands decrease and at shorter photolysis wavelengths both sites disappear and ClOO is observed as photoproduct. All vibrational data of the new species are collected in Table 11. The band positions and relative intensities as well as the $^{35/37}Cl$ isotopic shift of the latter four bands are very similar to the spectrum of $FClO_3$ (ν_i, $\Delta\nu_i$ $^{35/37}Cl$, int.: 1316, 19, vs; 1062, 3, m; 712, 10, s; 588, 3 cm^{-1}, m). Hence, the new radical O_3ClO-O_2 has been formed, which is comparable to the recently described isoelectronic species FSO_2O-O_2.[218] Both new peroxy radicals will be investigated in detail in a future matrix study.

The UV/Vis spectrum of ClO_4: Our experimental setup allows the measurement of IR and UV/Vis spectra from the same matrix, which guaranties that the same absorber correlates in both spectral regions. The corresponding UV/Vis spectra of the five best low pressure flash thermolysis experiments of Cl_2O_6 are used to "extract" the UV spectrum of ClO_4 from the raw data. For this purpose reference spectra of Cl_2O_6, ClO_3 and ClO_2 are used to subtract their content in the raw spectra. Finally the raw spectra are averaged and smoothed in the region 370 to 420 nm, because in this region incompensations by subtraction of ClO_2 bands appeared. Below 370 nm no reliable absorption profile can be evaluated, due to strongly absorbing by-products. The resulting spectrum is shown in Figure 14.

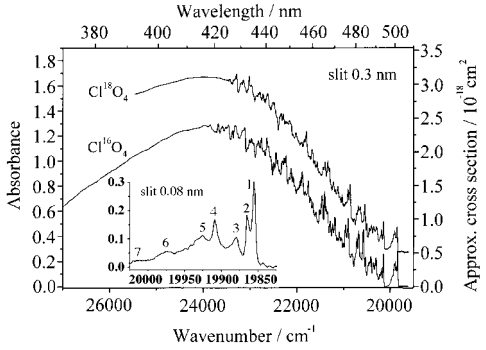

Figure 14. UV/Vis spectrum of ClO_4 isolated in a neon matrix. The spectrum of $Cl^{18}O_4$ is shifted up by 0.3 absorbance units. Bands of ClO_2 are subtracted in the region $\lambda > 420-430$ nm. For $\lambda < 420-430$ nm the spectrum is smoothed (see text). In the insert a high resolution spectrum of the onset is shown.

In Figure 15 an expanded scale spectrum including the spectrum of the ^{18}O isotope enriched species are shown. For the subtraction of the by-products $Cl^{16/18}O_2$ and $Cl^{16/18}O_3$ separate thermolysis experiments with $Cl_2{}^{16/18}O_6$ at higher

0947-6539/02/0824-5616 $ 20.00+.50/0 *Chem. Eur. J.* **2002**, *8*, No. 24

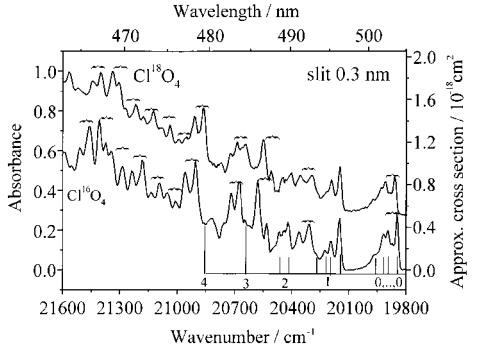

Figure 15. UV/Vis spectrum of ClO_4 isolated in a neon matrix in expanded scale, showing the overlying vibrational bands. Brackets indicate peaks shifted by about 50 cm^{-1} (see text, Table 15). The assignment of some peaks to a progression is shown by the vertical lines.

temperatures are performed, so that the amount of by-products [see Eqs. (7.2), (41) – (43)] is enhanced. The resulting $Cl^{18}O_4$ spectrum is somewhat disturbed by $Cl^{16}O^{18}O_3$ isotopomers (see above). The absorption cross section scale in Figures 14 and 15 is estimated from the ClO_2 absorbance at 420.58 nm (4,0,0 transition) in the raw spectra and its known cross section[23] assuming a band width similar to that of gaseous ClO_2 at room temperature, and assuming a 1 : 1 mixture of ClO_2 : ClO_4 according to Equation (7.2).

Above 510 nm no absorption is observed, which is in accordance with the photoelectron spectrum of the ClO_4^- anion[25] where no electron detachments between 1 and 2.5 eV (20000 cm^{-1}) above the X^2B_1 ground state are detectable. The UV/Vis spectrum of ClO_4 shows a strongly structured band with a maximum at about 23500 cm^{-1}, a half width of about 5000 cm^{-1} and a band origin at 19847 cm^{-1} for $Cl^{16}O_4$. The reproducible fine structure on the long wavelength wing is most unusual on three accounts: i) the 0 – 0 transition line consists of seven components as displayed in the insert of in Figure 14; ii) the 0 – 0 transition of $Cl^{16}O_4$ is about 12 cm^{-1} lower in energy, than that of $Cl^{18}O_4$ (uncertainty of the difference is ± 5 cm^{-1}) and iii) the fine structure is very complex.

Splittings of bands due to electronic transition are not unexpected in the matrix. They can amount to 30 – 70 cm^{-1} as measured for FCO_2[159] in a Ne matrix or for ClO_2[190] in a Ar matrix. However, the separations between the bands in the insert in Figure 14 are 10, 24, 55, 70, 117, and 155 cm^{-1} (0.08 nm slit). As discussed in the preceding section, a portion of ClO_4 in the C_s form can be recognized; the two satellites (117, 155 cm^{-1}) can be caused by some ClO_4 distorted to the less stable C_s structure in two matrix cages. Furtheron, the separation between the first and the fourth band (≈50 cm^{-1}, 0.3 nm slit) in the 0 – 0 transition seem to be the main feature in the fine structure, as it appears at other band groups, also indicated by brackets in Figure 15. Unfortunately, the contour of the 0 – 0 transition is nearly faded out in the rest of the spectrum. Only the first progression can be analysed in some detail, supported by its contour (1,0; and 2,0) and further bands from the second derivative spectrum. This transition can be analysed up to the quantum number 4 (see Figure 15, Table 15) and a quadratic fit results in Equations (47) and (48).

Table 15. Positions of some progression bands of Ne matrix isolated ClO_4 in the $A^2B \leftarrow X^2A$ transition.

Site	$Cl^{16}O_4$	$Cl^{18}O_4$	Assignment
	wavenumber/cm^{-1}		
1,2	19847	19859	0,...,0
4	19895	19906	0,...,0
5	19918	19930	0,...,0
6	19972	19972	0,...,0
1,2	20147	20147	1,0
4	20193	20190	1,0
5	20227	20214	1,0
6	20270	20257	1,0
1,2	20415	20400	2,0
4	20469	20450	2,0
5	20494	20475	2,0
1,2	20640sh	20601sh	3,0
1,2	20840sh	20807sh	4,0
1,2	20307	20288	0,1 ?
4	20362	20356	0,1 ?
5	20387sh		0,1 ?
1,2	20672	20640	0,2 ?
4,5	20717	20684	0,2 ?
1,2	20905	20859	0,3 ?
4,5	20964	20908	0,3 ?
1,2	21090	21037	0,4 ?
4,5	21137	21077	0,4 ?
1,2	21182	21124	0,5 ?
4,5	21238	21177	0,5 ?
1,2	21286	21218	?
4,5	21340	21265	?
1,2	21456	21402	?
4,5	21512	21445	?
1,2	20532	20507	inverted
4,5	20576	20547	intensity
1,2	21011	20955	inverted
4,5	21050	20990	intensity
1,2	21374	21299	inverted
4,5	21409	21340	intensity

$$Cl^{16}O_4: \nu = 19847\ (\pm 1) + 320\ (\pm 1)\cdot N - 18\ (\pm 0.3)\cdot N^2 \quad (47)$$

$$Cl^{18}O_4: \nu = 19859\ (\pm 1) + 304\ (\pm 1)\cdot N - 16\ (\pm 0.2)\cdot N^2 \quad (48)$$

Theoretical calculations examine a $^2B_1$ ground state and an $^2A_2$ excited state[134] so that all a_1 and b_2 vibrations are allowed as progression bands.[212] Taking the relative isotopic shift of $Cl^{16/18}O_4$ into account the ν_2 (a_1) vibration belongs to this progression, which is lowered by 64 % in the excited state. This vibrational motion is described as the symmetric stretching of the longer Cl–O bonds. Furthermore, the intensity is strongly decreased (analyzed by subtracting the totally smoothed spectrum from the original spectrum), which point to a continuum at quantum numbers higher than five.

Assignment of the other transitions is difficult to perform and must be tentative due to the possibility of combined progression. The data for progression bands up to 21500 cm^{-1} are gathered in Table 15 and taken from the second derivative spectrum. In comparison to the UV/Vis spectrum of ClO_4 the spectrum of isoelectronic SO_4^-[219, 220] is structureless and red-shifted by about 25 nm with a cross section of 6.3×10^{-18} cm^2 at 440 – 450 nm, which is about three times greater than our estimated cross section of ClO_4. Furthermore a high energy band of lower intensity is observed at about 320 nm in the UV/Vis spectrum of SO_4^-. In this region our spectrum is strongly perturbed by ClO_2 and/or $(OClO)_2$.

  0947-6539/02/0824-5617 $ 20.00+.50/0

The Photochemistry of ClO_4: Light of wavelengths >495 nm is sufficient to deplete Ne matrix isolated ClO_4. The only detectable IR active product is OClO and therefore the photolysis should proceed as follows [Eq. (49)].

$$ClO_4 \xrightarrow{h\nu \geq 495\,nm} OClO + O_2 \quad (49)$$

It is assumed that this photodissociation is a one-step process in the $A^2A_2 \leftarrow X^2B_1$ transition where the symmetric stretching of the longer ClO bonds is active, strongly decreased in energy and follow the proper coordinate.

ClO_4 isolated in an oxygen matrix seems to be more photostable. Light of wavelengths >395 nm is needed for the photolysis of the more photolabile matrix site and light of wavelengths <395 nm is suitable for photolysing both matrix sites. In both cases secondary photoisomerization of OClO to ClOO occurs.

Conclusion

The spectroscopic, bonding, structural and chemical properties of the radicals ClO_x ($x=1-4$) are very unusual in many respects. Especially ClO_4 stands out among these species. Due to a strong Jahn–Teller effect two of the ClO bonds are stretched leading to a C_{2v} equilibrium configuration. The C_s distorted geometry is found to be only a few kJ mol^{-1} higher in energy. The results of several recent ab initio calculations[38–40, 133, 134] are in accordance with the observed IR spectrum of ClO_4. A reason for the unusual broad IR bands is seen in the shallow potential which makes the ClO_4 radical floppy. Also the photochemistry of ClO_4 differs from that of the other radicals. While ClO_x ($x=1-3$) photodissociate, primarily into ClO_{x-1}+O the ClO_4 radical yields ClO_2+O_2. Irregularities of the properties of the chlorine oxide radicals with increasing oxidation numbers are seen in: i) the energy onset for photodissociation follows the sequence $ClO_3 < ClO_4 < ClO_2 < ClO$ and consequently ClO_3 is the least and ClO the most photostable species; ii) dimerization leads for ClO to different unstable Cl_2O_2 isomers, for OClO to weakly bonded dimers, for ClO_3 to stable asymmetric $O_2ClOClO_3$ and for ClO_4 to decomposition products (presumably to $Cl_2O_6 + O_2$); iii) ClO bond lengths and bond energies follow the sequence $ClO < ClO_3 < ClO_2$ and $ClO_3 < ClO_2 < ClO$, respectively. The only nearly even trend appears in the electron affinity (eV): ClO (2.5),[174] ClO_2 (2.15), ClO_3 (4.25), ClO_4 (5.25).[25] The very high electron affinity of ClO_4 may be one reason for its strong interaction with molecular oxygen under formation of the peroxy radical O_3ClO-O_2. However, the electron affinity of ClO_4 is apparently not sufficient to form a stable $O_2^+ClO_4^-$ salt, because the ionization enregy of dioxygen amounts 12.07 eV.[174]

In contrast, in the series of the anions ClO_x^- ($x=1-4$), which contain just one electron more than the respective radicals, their bonding properties are changing smoothly with increasing oxidation number. Their bond lengths (pm) and force constants (10^2 N m^{-1}) gradually changes in the series ClO^- (–/3.3), ClO_2^- (157/4.3), ClO_3^- (149/5.87), ClO_4^- (145/7.45)[199, 221] and their bond angles can be rationalized by the VSEPR rules.

Experimental Section

Caution: *Chlorine oxides and ozone are potentially explosive, especially in the presence of oxidizable materials. It is important to take proper safety precautions when these compounds are handled and reactions are carried out. Reactions involving either one of them should be carried out only with millimolar quantities.*

General procedures and reagents: Volatile materials were manipulated in a glass vacuum line equipped with two capacitance pressure gauges (221 AHS-1000 and 221 AHS-10 MKS Baratron, Burlington, MA), three U-traps, and valves with PTFE stems (Young, London, UK). The vacuum line was connected to an IR cell (optical path length 200 mm, Si windows 0.5 mm thick) contained in the sample compartment of a FTIR instrument. This allows one to observe the purification processes and to follow the course of reactions. The compounds ClO_2,[222] $HOClO_3$,[223] $ClOClO_3$,[224] $FOClO_3$,[225] ClO_2ClO_4[47, 86] and $ClONO_2$[226] were prepared according to literature procedures and stored in flame-sealed glass ampoules under liquid nitrogen in a storage Dewar vessel. By using an ampoule key[227] the ampoules were opened at the vacuum line, an appropriate amount was taken out for the experiments and then they were flame-sealed again. ^{18}O-labelled ClO_2 was prepared by treating ClF_3 with $D_2{}^{18}O$.[228] Isotopically enriched $^{18}O_3$ was synthesized from $^{18}O_2$ in a small home-made ozonizer.[229, 230] Excess of $^{18}O_2$ was recovered by cryopumping oxygen into a vessel filled with molecular sieve (5 Å) held at $-196\,^\circ$C. To prepare ^{18}O-enriched $CsClO_4$, CsCl was dissolved in $D_2{}^{18}O$ and oxidized by an excess of XeF_2 first at room temperature and then for 2 h at 80 °C. According to the literature the synthesis of the isotopically labelled $Cl_2{}^{18}O_6$ is accomplished by the reaction of $Cl^{18}O_2$ and $^{18}O_3$. Due to incomplete labelled precursors (ClO_2: 93 % $Cl^{18}O_2$, 6 % $Cl^{16}O^{18}O$, 1 % $Cl^{16}O_2$; O_3: 94 % $^{18}O_3$, 6 % other isotopomers) up to 20 % of $^{16/18}O_2Cl^{16}OCl^{18}O_3$ and other isotopomers were produced.

Chemicals: The following chemicals were obtained from commercial sources and used without purification: H_2SO_4 (96 %), $HClO_4$ (73 %), $KClO_3$, $KClO_4$, $CsClO_4$ (all p.a.: Merck, Darmstadt, Germany) $D_2{}^{18}O$ (98.97 % ^{18}O, Johnson Matthey, Alfa Products, Karlsruhe, Germany), F_2 (commercial grade, Solvay, Hannover, Germany), $^{18}O_2$ (99.5 %, Chemotrade, Düsseldorf, Germany), O_2 (99.999 %, Linde, München, Germany), Ar (99.999 %, Messer Griesheim, Krefeld, Germany) and Ne (>99,999 %, Messer Griesheim, Krefeld, Germany).

Preparation of the matrices: Small amounts of the samples (ca. 0.1 mmol) were transferred in vacuo into a small U-trap kept in liquid nitrogen. This U-trap was mounted in front of the matrix support (a metal mirror) and allowed to reach a temperature of $-130\,^\circ$C or $-120\,^\circ$C for ClO_2, $-105\,^\circ$C for $HOClO_3$ and $-38\,^\circ$C for Cl_2O_6 in cold bathes. In the temperature range -130 to $-110\,^\circ$C and -110 to $-30\,^\circ$C Dewar vessels filled with isopentane or ethanol were used, respectively. A gas stream (≈ 3 mmol h^{-1}) of argon, oxygen or neon was directed over the cold sample in the U-trap, and the resulting gas mixtures passed the heated quartz nozzle (∅ 4 mm with an end orifice of 1 mm) within milliseconds and were quenched on the matrix support at 12 or 5 K, respectively. Because the vapor pressures of the samples in the cold U-trap are of the magnitude of 10^{-3} mbar and the pressures of the inert gas streams during the deposition are about 1 mbar in the U-trap, the resulting sample to gas ratios can be estimated to be in the range 1:1000. In case of ClO_2 the higher temperatures enables greater sample to gas ratios and formation of an increased fraction of $(ClO_2)_2$ molecules during the quenching process. For each sample two different amounts of matrix material (≈ 1 and 3 mmol, respectively) were deposited through the heated nozzle at temperatures of 200 for ClO_2, 350–380 for $ClOClO_3$, 350 for $FOClO_3$, 240 for Cl_2O_6 400–450 for $HOClO_3$ and 420–450 °C for $ClONO_2$. Heating the ClO_2/inert gas stream was necessary for dissociation of evaporated $(ClO_2)_2$ molecules. Mixtures of NO_2: Ne (1:1000) were prepared in a stainless steel high-vacuum line and transferred via a stainless steel capillary to the heated nozzle, and quenched as a matrix at 5 K.

IR spectroscopy: Gas-phase IR spectra were recorded with a resolution of 2 cm^{-1} in the range of 4000–400 cm^{-1}, using a FTIR instrument (Nicolet, Impact 400 D, Madison,WI) which was directly coupled with the vacuum line. Matrix IR spectra were recorded on a Bruker IFS 66v/S FT spectrometer (Bruker, Karlsruhe, Germany) in the reflectance mode, using a transfer optic. A DTGS or MCT detector together with a KBr/Ge

0947-6539/02/0824-5618 $ 20.00+.50/0 *Chem. Eur. J.* **2002**, *8*, No. 24

beam splitter operated in the regions of 5000–400 or 7000–600 cm^{-1}, respectively. In these regions 64 scans were co-added for each spectrum using apodized resolutions of 1.0, 0.25 or 0.13 cm^{-1}. A far IR-DTGS detector together with a Ge coated 6 μm Mylar beam splitter was used in the region of 650–80 cm^{-1}. In this region 64 scans were co-added for each spectrum using an apodized resolution of 1.0 cm^{-1}.

UV/Vis spectroscopy: UV/Vis spectra were recorded in the region 200–750 nm with a Perkin–Elmer Lambda 900 instrument (Perkin–Elmer, Norwalk,CT) using a slit of 0.3 nm, data point separation of 0.15 nm and a integration time of 0.48 s for each datapoint in the range 200–490 (510 for ClO_4) nm. At higher wavelength a datapoint separation of 0.4 nm was used. For matrix measurements two 2 m long quartz single fibers with a special condensor optic (Hellma, Jena Germany) were used. Mercury and Neon pencil lamps were used for wavelength calibration (Oriel Instruments, Stratford, CT).

Photolysis experiments: These were performed on the matrices in the visible and UV regions by using a 250 W tungsten halogen lamp (Osram, München, Germany) or a high-pressure mercury lamp (TQ 150, Heraeus, Hanau, Germany), respectively, in combination with a water coold quartz condensor optic and cut off or interference filters (Schott, Mainz (Germany)). Details of the matrix apparatus have been described elsewhere.[159]

For analysis of the IR and UV/Vis matrix spectra of the pyrolysis products, a series of reference spectra of ClO_2, Cl_2O_4, Cl_2O_6, $FClO_4$, $HClO_4$, ClO and NO_2 have been measured. For FO_2 and F_2O_2 literature data were used.[1]

Acknowledgement

Financial support by the Deutsche Forschungsgemeinschaft and the Fonds der Chemischen Industrie is gratefully acknowledged. We thank S. v. Ahsen for assistance in ab initio computations and J. Francisco for helpful discussions and providing his unpublished paper on ClO_4.

[1] R. P. Wayne, G. Poulet, P. Biggs, J. P. Burrows, R. A. Cox, P. J. Crutzen, G. D. Hayman, M. E. Jenkin, G. Le-Bras, G. K. Moortgat, U. Platt, R. N. Schindler, *Atmos. Envir.* **1995**, *29*, 2675 and references therein.
[2] H. Grothe, H. Willner, *Angew. Chem.***1994**, *106*, 1581; *Angew. Chem. Int. Ed.* **1994**, *33*, 1482.
[3] H. Grothe, H. Willner, *Angew. Chem*. **1996**, *108*, 816; *Angew. Chem. Int. Ed.* **1996**, *35*, 768.
[4] J. Jacobs, M. Kronberg, H. S. P. Müller, H. Willner, *J. Am. Chem. Soc.* **1994**, *116*, 1106.
[5] H. S. P. Müller, H. Willner, *J. Chem. Phys.* **1993**, *97*, 10589.
[6] H. Davy, *Philos. Trans.* **1815**, *105*, 214.
[7] F. Stadion, *Ann. Chim. Phys.* **1818**, *8*, 406.
[8] J. L. Gay-Lussac, *Ann. Chim. Phys.* **1818**, *8*, 406.
[9] M. Faraday, *Philos. Trans.* **1823**, *113*, 189.
[10] E. Millon, *Justus Liebigs Annalen* **1843**, *46*, 281.
[11] W. Gerhartz, in *Ullmanns Encyclopedia of Industrial Chemistry*, *Vol. A6*, *5th complete rev. ed.*, Verlag Chemie, Weinheim, **1986**.
[12] A. E. Croce, J. E. Sicre, *Z. Phys. Chem.* **2000**, *214*, 533.
[13] A. Rehr, M. Jansen, *Inorg. Chem.* **1992**, *31*, 4740.
[14] A. Rehr, M. Jansen, *Angew. Chem.* **1991**, *103*, 1506; *Angew. Chem. Int. Ed.* **1991**, *30*, 1510.
[15] R. D. Harcourt, *J. Phys. Chem.* **1993**, *97*, 1351.
[16] H. Willner, unpublished results, **2002**.
[17] M. Tanoura, K. Chiba, K. Tanaka, T. Tanaka, *J. Mol. Spectrosc.* **1982**, *95*, 157.
[18] K. Miyazaki, M. Tanoura, K. Tanaka, T. Tanaka, *J. Mol. Spectrosc.* **1986**, *116*, 435.
[19] H. S. P. Müller, G. O. Sorensen, M. Birk, R. R. Friedl, *J. Mol. Spectrosc.* **1997**, *186*, 177.
[20] J. Ortigoso, R. Escribano, J. B. Burkholder, C. J. Howard, W. J. Lafferty, *J. Mol. Spectrosc.* **1991**, *148*, 346.
[21] J. Ortigoso, R. Escribano, J. B. Burkholder, W. J. Lafferty, *J. Mol. Spectrosc.* **1992**, *155*, 25.
[22] J. Ortigoso, R. Escribano, J. B. Burkholder, W. J. Lafferty, *J. Mol. Spectrosc.* **1993**, *158*, 347.
[23] A. Wahner, C. S. Tyndall, A. R. Ravishankara, *J. Phys. Chem.* **1987**, *91*, 2734.
[24] E. C. Richard, V. Vaida, *J. Phys. Chem.* **1991**, *94*, 153.
[25] X. B. Wang, L. S. Wang, *J. Chem. Phys.* **2000**, *113*, 10928.
[26] U. Rockland, H. Baumgärtel, E. Rühl, O. Lösking, H. S. P. Müller, H. Willner, *Ber. Bunsenges. Phys. Chem.* **1995**, *99*, 969.
[27] R. Flesch, E. Rühl, K. Hottmann, H. Baumgärtel, *J. Phys. Chem.* **1993**, *97*, 837.
[28] F. Zabel, *Ber. Bunsenges. Phys. Chem.* **1991**, *95*, 893.
[29] H. F. Davis, Y. T. Lee, *J. Phys. Chem.* **1992**, *96*, 5681.
[30] K. A. Peterson, H. J. Werner, *J. Chem. Phys.* **1996**, *105*, 9823.
[31] L. H. Lai, C. P. Liu, Y. P. Lee, *J. Chem. Phys.* **1998**, *109*, 988.
[32] Y. J. Chang, J. D. Simon, *J. Phys. Chem.* **1996**, *100*, 6406.
[33] R. C. Dunn, B. N. Flanders, J. D. Simon, *J. Phys. Chem.* **1995**, *99*, 7360.
[34] V. Stert, H. H. Ritze, E. T. J. Nibbering, W. Radloff, *Chem. Phys.* **2001**, *272*, 99.
[35] R. F. Delmdahl, D. H. Parker, A. T. J. B. Eppink, *J. Chem. Phys.* **2001**, *114*, 8339.
[36] C. J. Pursell, J. Conyers, P. Alapat, R. Parveen, *J. Phys. Chem.* **1995**, *99*, 10433.
[37] C. J. Pursell, J. Conyers, C. Denison, *J. Phys. Chem.* **1996**, *100*, 15450.
[38] M. Alcami, O. Mò, M. Yanez, I. L. Cooper, *J. Chem. Phys.* **2000**, *112*, 6131.
[39] A. Beltran, J. Andrès, S. Noury, B. Silvi, *J. Phys. Chem.* **1999**, *103*, 3078.
[40] R. Janoschek, *J. Mol. Struct.* (*Theochem*) **1998**, *423*, 219.
[41] K. A. Peterson, H. J. Werner, *J. Chem. Phys.* **1992**, *96*, 8948.
[42] E. P. Clifford, P. G. Wenthold, R. Gareyev, W. C. Lineberger, C. H. DePuy, V. M. Bierbaum, G. B. Ellison, *J. Chem. Phys.* **1998**, *109*, 10293.
[43] A. Popper, *Justus Liebigs Annalen* **1885**, *227*, 161.
[44] A. Popper, *Justus Liebigs Annalen* **1885**, *231*, 137.
[45] E. J. Bowen, *J. Chem. Soc.* **1923**, *123*, 2328.
[46] H. Booth, E. J. Bowen, *J. Chem. Soc.* **1925**, *127*, 510.
[47] M. Bodenstein, P. Harteck, E. Padelt, *Z. Anorg. Allg. Chem.* **1925**, *147*, 233.
[48] M. Bodenstein, G. Kistiakowski, *Z. Phys. Chem.* **1925**, *116*, 371.
[49] H. J. Schumacher, C. Wagner, *Z. Phys. Chem.* **1929**, *B5*, 199.
[50] M. Bodenstein, E. Padelt, H. J. Schumacher, *Z. Phys. Chem.* **1929**, *B5*, 209.
[51] C. F. Goodeve, J. I. Wallace, *Trans. Faraday Soc.* **1930**, *26*, 254.
[52] E. J. Bowen, W. M. Cheung, *J. Chem. Soc.* **1932**, *132*, 1200.
[53] H. C. Urey, H. C. Bates, *Phys. Rev.* **1929**, *34*, 1541.
[54] G. Pannetier, A. G. Gaydon, *Nature* **1948**, *161*, 242.
[55] Z. G. Szabò, *J. Chem. Soc.* **1950**, 1356.
[56] Z. G. Szabò, *Acta Univ. Szegediensis Acta Chem. Phys.* **1950**, *3*, 20.
[57] P. Huhn, F. Tudos, Z. G. Szabò, *Magyar Tudomànyos Akad. Kèm. Osztàlyànak Közlemènyei* **1954**, *5*, 409 [*Chem. Abstr.* **1954**, *50*, 41e].
[58] R. G. W. Norrish, G. H. J. Neville, *J. Chem. Soc.* **1934**, 1864.
[59] R. G. W. Norrish, G. Porter, *Nature* **1949**, *164*, 658.
[60] G. Porter, *Proc. Roy. Soc. Lond. Ser. A* **1950**, *200*, 284.
[61] G. Porter, *Disc. Faraday Soc.* **1950**, *9*, 60.
[62] G. Porter, F. J. Wright, *Disc. Faraday Soc.* **1953**, *14*, 23.
[63] F. J. Lipscomb, R. G. W. Norrish, B. A. Thrush, *Proc. Roy. Soc. Lond. Ser. A* **1955**, *233*, 455.
[64] F. H. C. Edgecombe, R. G. W. Norrish, B. A. Thrush, *Proc. Roy. Soc. Lond. Ser. A* **1957**, *243*, 24.
[65] H. S. Johnston, E. D. Morris, J. van de Bogaerde, *J. Am. Chem. Soc.* **1969**, *91*, 7712.
[66] M. Mandelmann, R. W. Nicholls, *J. Quant. Spectrosc. Radiat. Transfer* **1976**, *17*, 483.
[67] J. L. Jourdain, G. Le Bras, G. Poulet, J. Combourieu, R. Rigaud, B. Leroy, *Chem. Phys. Lett.* **1978**, *57*, 109.
[68] R. A. Barton, R. A. Cox, T. J. Wallington, *J. Chem. Soc. Faraday Trans. 1* **1984**, *80*, 2737.
[69] S. P. Sander, R. R. Friedl, *J. Phys. Chem.* **1989**, *93*, 4764.
[70] F. G. Simon, W. Schneider, G. K. Moortgat, J. P. Burrows, *J. Photochem. Photobio. A* **1990**, *55*, 1.

  0947-6539/02/0824-5619 $ 20.00+.50/0

[71] L. T. Molina, F. S. Rowland, *Nature* **1974**, *249*, 810.
[72] L. T. Molina, M. J. Molina, *J. Phys. Chem.* **1987**, *91*, 433.
[73] L. M. Avallone, D. W. Toohey, *J. Geophys. Res. Atmos.* **2001**, *106*, 10411.
[74] P. Solomon, J. Barrett, B. Connor, S. Zoonematkermani, A. Parrish, A. Lee, J. Pyle, M. Chipperfield, *J. Geophys. Res.* **2000**, *105*, 28979.
[75] G. P. Bonne, R. M. Stimpfle, R. C. Cohen, P. B. Voss, K. K. Perkins, J. G. Anderson, R. J. Salawitch, J. W. Elkins, G. S. Dutton, K. W. Jucks, G. C. Toon, *J. Geophys. Res. Atmos.* **2000**, *105*, 1957.
[76] L. K. Randeniya, I. C. Plumb, K. R. Ryan, *J. Geophys. Res. Atmos.* **1999**, *104*, 26667.
[77] B. Sen, G. B. Ostermann, R. J. Salawitch, G. C. Toon, J. J. Margitan, J. F. Blavier, A. Y. Chang, R. D. May, C. R. Webster, R. M. Stimpfle, G. P. Bonne, P. B. Voss, K. K. Perkins, J. G. Anderson, R. C. Cohen, J. W. Elkins, G. S. Dutton, D. F. Hurst, P. A. Romashkin, E. L. Atlas, S. M. Schauffler, M. Loewenstein, *J. Geophys. Res. Atmos.* **1999**, *104*, 26656.
[78] R. M. Stimpfle, R. C. Cohen, G. P. Bonne, P. B. Voss, K. K. Perkins, L. C. Koch, J. G. Anderson, R. J. Salawitch, S. A. Lloyd, R. S. Gao, L. A. Del Negro, E. R. Keim, T. P. Bui, *J. Geophys. Res. Atmos.* **1999**, *104*, 26705.
[79] L. Jaegle, Y. L. Yung, G. C. Toon, B. Sen, J. F. Blavier, *Geophys. Res. Lett.* **1996**, *23*, 1749.
[80] G. P. Knight, T. Beiderhase, F. Helleis, G. K. Moortgat, J. N. Crowley, *J. Phys. Chem. A* **2000**, *104*, 1674.
[81] B. J. Drouin, C. E. Miller, E. A. Cohen, G. Wagner, M. Birg, *J. Mol. Spectrosc.* **2001**, *207*, 4.
[82] M. Bodenstein, H. J. Schumacher, *Z. Phys. Chem.* **1929**, *B5*, 233.
[83] G. K. Rollefson, A. C. Byrns, *J. Am. Chem. Soc.* **1934**, *56*, 364.
[84] A. C. Byrns, G. K. Rollefson, *J. Am. Chem. Soc.* **1934**, *56*, 1250.
[85] A. C. Byrns, G. K. Rollefson, *J. Am. Chem. Soc.* **1934**, *56*, 2245.
[86] H. J. Schumacher, G. Stieger, *Z. Anorg. Allg. Chem.* **1929**, *184*, 272.
[87] C. F. Goodeve, F. A. Todd, *Nature* **1933**, *132*, 514.
[88] M. H. Kalina, J. W. T. Spinks, *Can. J. Res.* **1938**, *16B*, 381.
[89] C. F. Goodeve, F. D. Richardson, *J. Chem. Soc.* **1937**, 294.
[90] C. F. Goodeve, F. D. Richardson, *Trans. Faraday Soc.* **1937**, *33*, 453.
[91] J. Farquharson, C. F. Goodeve, F. D. Richardson, *Trans. Faraday Soc.* **1936**, *32*, 790.
[92] L. Pauling, L. O. Brockway, *J. Am. Chem. Soc.* **1937**, *59*, 13.
[93] H. C. Longuet-Higgins, *Nature* **1944**, *153*, 408.
[94] H. A. Lehmann, G. Krüger, *Z. Anorg. Allg. Chem.* **1953**, *274*, 141.
[95] M. Schmeisser, *Angew. Chem.* **1955**, *67*, 493.
[96] V. N. Belevskii, L. T. Bugaenko, *Russ. J. Inorg. Chem.* **1967**, *12*, 1203.
[97] V. A. Nevostruev, Y. Zakharov, I. F. Kolesnikova, *Izv.Tomsk. Politekh. Inst.* **1970**, *176*, 111 [*Chem. Abstr.* **1970**, *75*, 124929c].
[98] C. J. Schack, K. O. Christe, *Inorg. Chem.* **1974**, *13*, 2378.
[99] K. M. Tobias, M. Jansen, *Angew. Chem.* **1986**, *98*, 994; *Angew. Chem. Int. Ed.* **1986**, *25*, 993.
[100] K. M. Tobias, M. Jansen, *Z. Anorg. Allg. Chem.* **1987**, *550*, 16.
[101] M. Jansen, G. Schatte, K. M. Tobias, H. Willner, *Inorg. Chem.* **1988**, *27*, 1703.
[102] M. Jansen, K. M. Tobias, H. Willner, *Naturwissenschaften* **1986**, *73*, 734.
[103] M. I. Lòpez, J. E. Sicre, *J. Phys. Chem.* **1990**, *94*, 3860.
[104] A. J. Arvia, W. H. Basualdo, H. J. Schumacher, *Z. Anorg. Allg. Chem.* **1956**, *286*, 58.
[105] R. V. Figini, E. Coloccia, H. J. Schumacher, *Z. Phys. Chem. Neue Folge* **1958**, *14*, 32.
[106] V. Handwerk, R. Zellner, *Ber. Bunsenges. Phys. Chem.* **1986**, *90*, 92.
[107] A. J. Colussi, *J. Phys. Chem.* **1990**, *94*, 8922.
[108] A. J. Colussi, R. W. Redmond, J. C. Scaiano, *J. Phys. Chem.* **1989**, *93*, 4783.
[109] A. J. Colussi, S. P. Sander, R. R. Friedl, *J. Phys. Chem.* **1992**, *96*, 4442.
[110] J. F. Gleason, F. L. Nesbitt, L. J. Stief, *J. Phys. Chem.* **1994**, *98*, 126.
[111] W. Wongdontri-Stuper, R. K. M. Jayanty, R. Simonaites, J. Heicklen, *J. Photochem.* **1979**, *10*, 163.
[112] S. S. Prasad, W. M. Adams, *J. Photochem.* **1980**, *13*, 243.
[113] R. W. Davidson, D. G. Williams, *J. Phys. Chem.* **1973**, *77*, 2515.
[114] J. W. Birks, B. Shoemaker, T. J. Leck, R. A. Borders, L. J. Hart, *J. Chem. Phys.* **1977**, *66*, 4591.
[115] T. Rathmann, R. N. Schindler, *Ber. Bunsenges. Phys. Chem.* **1992**, *96*, 421.
[116] T. Rathmann, R. N. Schindler, *Chem. Phys. Lett.* **1992**, *190*, 539.
[117] A. Rauk, E. Tschuikow-Roux, Y. Chen, M. P. McGrath, L. Radom, *J. Phys. Chem.* **1993**, *97*, 7947.
[118] M. A. Workmann, J. S. Francisco, *Chem. Phys. Lett.* **1997**, *279*, 158.
[119] R. Escribano, R. G. Mosteo, P. C. Gòmez, *Can. J. Phys.* **2001**, *79*, 597.
[120] M. Domae, Y. Katsumara, P. Y. Jiang, R. Nagaishi, C. Hasegawa, K. Ishigure, Y. Yoshida, *J. Phys. Chem.* **1994**, *98*, 190.
[121] M. Domae, Y. Katsumara, P. Y. Jiang, R. Nagaishi, K. Ishigure, T. Kozawa, Y. Yoshida, *J. Chem. Soc. Faraday Trans.* **1996**, *92*, 2245.
[122] Z. Zuo, Y. Katsumara, K. Ueda, K. Ishigure, *J. Chem. Soc. Faraday Trans.* **1997**, *93*, 533.
[123] M. Gomberg, *J. Am. Chem. Soc.* **1923**, *45*, 398.
[124] M. Gomberg, H. R. Gamrath, *Trans. Faraday Soc.* **1934**, *30*, 24.
[125] L. V. Pisarzhevskii, *Bull. Acad. Sci. USSR Classe Sci. Math. Nat.* **1933**, *8*, 1121 [*Chem. Abstr.* **1933**, *28*, 2636[1]].
[126] L. Birckenbach, J. Goebeau, *Ber.* **1932**, *65*, 395.
[127] R. N. Hazeldine, A. G. Sharpe, *J. Chem. Soc.* **1952**, 993.
[128] E. Weitz, *Angew. Chem.* **1954**, *66*, 658.
[129] K. O. Christe, C. J. Schack, *Inorg. Chem.* **1974**, *11*, 1682.
[130] I. P. Fisher, *Trans. Faraday Soc.* **1968**, *64*, 1852.
[131] R. Simonaites, J. Heicklen, *Planet. Space Sci.* **1975**, *23*, 1567.
[132] H. Schmidt, J. Noack, *Z. Anorg. Allg. Chem.* **1958**, *296*, 262.
[133] T. J. Van Huis, H. F. Schaefer III, *J. Chem. Phys.* **1996**, *106*, 4028.
[134] M. A. Workmann, J. S. Francisco, personal communication, **2002**.
[135] M. I. Lòpez, A. E. Croce, J. E. Sicre, *J. Photochem. Photobio. A: Chemistry* **1998**, *112*, 97.
[136] T. Cole, *J. Chem. Phys.* **1961**, *35*, 1169.
[137] P. W. Atkins, J. A. Brivati, M. C. R. Keen, M. C. R. Symons, P. A. Trevalion, *J. Chem. Soc.* **1962**, 4785.
[138] J. R. Morton, *J. Chem. Phys.* **1966**, *45*, 1800.
[139] J. R. Byberg, S. J. K. Jensen, *J. Chem. Phys.* **1970**, *52*, 5902.
[140] O. Vinther, *J. Chem. Phys.* **1972**, *57*, 183.
[141] K. Shimokoshi, Y. Mori, *J. Phys. Chem.* **1973**, *77*, 3058.
[142] J. R. Byberg, J. Linderberg, *Chem. Phys. Lett.* **1975**, *33*, 612.
[143] J. R. Byberg, *Chem. Phys. Lett.* **1978**, *56*, 130.
[144] J. R. Byberg, *J. Chem. Phys.* **1981**, *75*, 2663.
[145] N. Bjerre, J. R. Byberg, *J. Chem. Phys.* **1984**, *82*, 2206.
[146] J. R. Byberg, *J. Phys. Chem.* **1995**, *99*, 13392.
[147] J. R. Byberg, *J. Phys. Chem.* **1996**, *100*, 9247.
[148] B. G. Hegde, A. Rastogi, R. Damle, R. Chandramani, S. V. Bhat, *J. Phys. Condens. Matter* **1997**, *9*.
[149] M. Yavuz, A. Bulut, H. Kalkan, E. Öztekin, *ARI: an interdiciplinary journal of physical and engineering science* **1998**, *51*, 6.
[150] M. Yavuz, *Radiat. Phys. Chem.* **1999**, *54*, 143.
[151] B. G. Hegde, A. Anand, S. V. Bhat, *Appl. Magn. Reson.* **2000**, *19*, 111.
[152] M. J. Almond, A. J. Downs, *Adv. Spectrosc.* **1989**, *17*, 1.
[153] H. Schnöckel, H. Willner, in *Infrared and Raman Soectroscopy* (Ed.: B. Schrader), Verlag Chemie, Weinheim, **1995**, pp. 297.
[154] A. Lester, in *Chemistry and physics of matrix-isolated-species* (Eds.: A. Lester, M. Moskovits), Elsevier, New York, **1989**, pp. 1.
[155] P. Bruckmann, H. Willner, *Environ. Sci. Technol.* **1983**, *17*, 352.
[156] G. A. Argüello, H. Willner, *J. Phys. Chem. A* **2001**, *105*, 3466.
[157] R. Kopitzky, H. Willner, H. G. Mack, A. Pfeiffer, H. Oberhammer, *Inorg. Chem.* **1998**, *37*, 6208.
[158] S. Sander, H. Pernice, H. Willner, *Chem. Eur. J.* **2000**, *6*, 3645.
[159] G. A. Argüello, H. Grothe, M. Kronberg, H. Willner, *J. Phys. Chem.* **1995**, *99*, 17525.
[160] B. Casper, H. G. Mack, H. S. P. Müller, H. Willner, H. Oberhammer, *J. Phys. Chem.* **1994**, *98*, 8339.
[161] A. J. Colussi, M. A. Grela, *J. Phys. Chem.* **1993**, *97*, 3775.
[162] M. A. Grela, A. J. Colussi, *J. Phys. Chem.* **1996**, *100*, 10150.
[163] D. R. Goddard, E. D. Hughes, C. K. Ingold, *Nature* **1946**, *158*, 480.
[164] A. Simon, H. Borrmann, *Angew. Chem.* **1988**, *100*, 1386; *Angew. Chem. Int. Ed.* **1988**, *27*, 1339.
[165] A. Simon, H. Borrmann, *Z. Kristallogr.* **1988**, *185*, 470.
[166] C. J. Cobos, A. E. Croce, E. Castellano, *J. Photochem. Photobio. A: Chemistry* **1994**, *84*, 101 and references therein.
[167] H. W. Jochims, W. Denzer, H. Baumgärtel, O. Lösking, H. Willner, *Ber. Bunsenges. Phys. Chem.* **1992**, *96*, 573.
[168] K. Johnsson, A. Engdahl, J. Kölm, J. Nieminen, B. Nelander, *J. Phys. Chem.* **1995**, *99*, 3902.
[169] V. I. Lang, S. P. Sander, R. R. Friedl, *J. Mol. Spectrosc.* **1988**, *132*, 89.

0947-6539/02/0824-5620 $ 20.00+.50/0 *Chem. Eur. J.* **2002**, *8*, No. 24

[170] J. B. Burkholder, P. D. Hammer, C. J. Howard, A. Goldmann, *J. Geophys. Res.* **1989**, *94*, 2225.
[171] R. S. Rogowski, C. H. Bair, W. R. Wade, J. M. Hoell, G. E. Copeland, *Appl. Opt.* **1978**, *17*, 1301.
[172] J. B. Burkholder, P. D. Hammer, C. J. Howard, A. G. Maki, G. Thompson, C. Chackerian Jr., *J. Mol. Spectrosc.* **1987**, *124*, 139.
[173] A. J. Barnes, in *Vibrational Spectroscopy of Trapped Species* (Ed.: H. E. Hallam), Wiley, London, **1973**.
[174] K. P. Huber, G. Herzberg, *Molecular Spectra and Molecular Structure*, *Vol. 4*, *Constants of Diatomic Molecules*, Van Nostrand Reinhold, New York, **1979**.
[175] F. K. Chi, L. Andrews, *J. Phys. Chem.* **1973**, *77*, 3062.
[176] L. Andrews, J. Raymond, *J. Chem. Phys.* **1971**, *55*.
[177] M. M. Rochkind, G. C. Pimentel, *J. Chem. Phys.* **1967**, *46*, 4481.
[178] W. G. Alcock, G. C. Pimentel, *J. Chem. Phys.* **1968**, *48*.
[179] T. Fängström, D. Edvardsson, M. Ericsson, S. Lunell, C. Enkvist, *Int. J. Quant. Chem.* **1998**, *66*, 203.
[180] Y. K. Han, K. H. Kim, Y. S. Lee, K. K. Baeck, *J. Mol. Struct.* (*Theochem*) **1998**, *431*, 185.
[181] T. J. Lee, C. M. Rohlfing, J. E. Rice, *J. Chem. Phys.* **1992**, *97*, 6593.
[182] M. P. McGrath, K. C. Clemitshaw, F. S. Rowland, W. J. Hehre, *J. Phys. Chem.* **1990**, *94*, 6126.
[183] H. S. P. Müller, H. Willner, *Ber. Bunsenges. Phys. Chem.* **1992**, *96*, 427.
[184] H. S. P. Müller, Ph. D. thesis, Universität Hannover (Germany), **1992**.
[185] M. Birk, R. R. Friedl, E. A. Cohen, H. M. Pickett, S. P. Sander, *J. Chem. Phys.* **1989**, *91*, 6588.
[186] U. Kirchner, T. Benter, R. N. Schindler, in *Ozonforschungsprogramm*, *Research Report*, **1994**, pp. 320.
[187] A. Arkell, I. Schwager, *J. Am. Chem. Soc.* **1967**, *89*, 5999.
[188] K. Johnsson, A. Engdahl, B. Nelander, *J. Phys. Chem.* **1993**, *97*, 9603.
[189] J. D. Graham, J. T. Roberts, L. D. Anderson, V. H. Grassian, *J. Phys. Chem.* **1996**, *100*, 19551.
[190] C. P. Liu, L. H. Lai, Y. Y. Lee, S. C. Hung, Y. P. Lee, *J. Chem. Phys.* **1998**, *109*, 977.
[191] C. Breheny, G. Hancock, C. Morell, *Z. Phys. Chem.* **2001**, *215*, 305.
[192] M. K. W. Ko, N.-D. Sze, J. M. Rodriguez, D. K. Weistenstein, C. w. Heisey, R. P. Wayne, P. Biggs, C. E. Canosa-Mas, H. W. Sidebottom, J. Treacy, *Geophys. Res. Lett.* **1994**, *21*, 101.
[193] K. Nakamoto, *Infrared and Raman Spectra of Inorganic and Coordination Compounds*, 4th ed., Wiley, New York, **1986**.
[194] J. C. Decius, *J. Chem. Phys.* **1948**, *16*, 1025.
[195] H. J. Becher, *Fortschr. Chem. Forsch.* **1968**, *10*, 156.
[196] A. W. Richardson, R. W. Redding, J. C. D. Brand, *J. Mol. Spectrosc.* **1969**, *29*, 93.
[197] D. Christe, *J. Mol. Struct.* **1978**, *48*, 101.
[198] M. Sugie, M. Ayabe, H. Takeo, C. Matsumura, *J. Mol. Struct.* **1995**, *352/353*, 259.
[199] H. Siebert, *Anwendungen der Schwingungsspektroskopie in der anorganischen Chemie*, Springer, Berlin, **1966**.
[200] M. Nakata, M. Sugie, H. Takeo, C. Matsumura, T. Fukuyama, K. Kuchitsu, *J. Mol. Spectrosc.* **1981**, *86*, 241.
[201] C. M. Deeley, I. M. Mills, *J. Mol. Spectrosc.* **1985**, *114*, 368.
[202] C. M. Deeley, *J. Mol. Spectrosc.* **1987**, *122*, 481.
[203] H. S. P. Müller, E. A. Cohen, *J. Chem. Phys.* **2002**, *116*, 2407.
[204] H. S. P. Müller, E. A. Cohen, D. Christen, *J. Chem. Phys.* **1999**, *110*, 11865.
[205] H. S. P. Müller, *J. Mol. Struct.* **2000**, *517–518*, 335.
[206] A. G. Robiette, C. R. Parent, M. C. L. Gerry, *J. Mol. Spectrosc.* **1981**, *86*, 455.
[207] H. S. P. Müller, M. C. L. Gerry, *J. Mol. Spectrosc.* **1996**, *175*, 120.
[208] M. M. Maricq, J. J. Szente, *J. Phys. Chem.* **1992**, *96*, 4925.
[209] A. D. Kirshenbaum, A. G. Streng, *J. Chem. Phys.* **1961**, *35*, 1440.
[210] Y. Li, J. S. Francisco, *J. Chem. Phys.* **2000**, *112*, 8866.
[211] W. B. DeMore, S. P. Sander, D. M. Golden, R. F. Hampson, M. J. Kurylo, C. J. Howard, A. R. Ravishankara, C. E. Kolb, M. J. Molina, *Chemical kinetics and photochemical data for use in stratospheric modelling*, *Vol. 97–4*, NASA, Jet Propulsion Laboratory, Pasadena, California, **1997**.
[212] F. Engelke, *Aufbau der Moleküle*, Teubner, Stuttgart, **1985**.
[213] G. Herzberg, *Electronic Spectra of Polyatomic Molecules*, Van Nostrand, New York, **1966**.
[214] H. Herrmann, A. Reese, R. Zellner, *J. Mol. Struct.* **1995**, *348*, 183.
[215] E. Y. Misochko, A. V. Akimov, C. A. Wight, *J. Phys. Chem. A* **1999**, *103*, 7972.
[216] GAUSSIAN 98, Rev. A.5, M. J. Frisch, G. W. Trucks, H. B. Schlegel, G. E. Scuseria, M. A. Robb, J. R. Cheeseman, V. G. Zakrzewski, J. J. A. Montgomery, R. E. Stratmann, J. C. Burant, S. Dapprich, J. M. Millam, A. D. Daniels, K. N. Kudin, M. C. Strain, O. Farkas, J. Tomasi, V. Barone, M. Cossi, R. Cammi, B. Mennucci, C. Pomelli, C. Adamo, S. Clifford, J. Ochterski, G. A. Petersson, P. Y. Ayala, Q. Cui, K. Morokuma, D. K. Malick, A. D. Rabuck, K. Raghavachari, J. B. Foresman, J. Cioslowski, J. V. Ortiz, B. B. Stefanov, G. Liu, A. Liashenko, P. Piskorz, I. Komaromi, R. Gomperts, R. L. Martin, D. J. Fox, T. Keith, M. A. Al-Laham, C. Y. Peng, A. Nanayakkara, C. Gonzalez, M. Challacombe, P. M. W. Gill, B. Johnson, W. Chen, M. W. Wong, J. L. Andres, C. Gonzalez, M. Head-Gordon, E. S. Replogle, J. A. Pople, Gaussian Inc., Pittsburgh PA, **1998**.
[217] A. Arkell, *J. Am. Chem. Soc.* **1965**, *87*, 4057.
[218] A. E. Croce, C. J. Cobos, E. Castellano, *J. Fluorine Chem.* **1997**, *82*, 91.
[219] G. V. Buxton, S. McGowan, J. E. Salmon, J. E. Williams, N. D. Wood, *Atmos. Environ.* **1996**, *30*, 2483 and references therein.
[220] H. Herrmann, A. Reese, R. Zellner, in *Annual EUROTRAC Report* (Ed.: P. Borell), Brüssel, **1994**, pp. 61.
[221] H. J. Becher, F. Friedrich, H. Willner, *Z. Anorg. Allg. Chem.* **1976**, *426*, 15.
[222] G. Gordon, R. G. Kiefer, D. H. Rosenblatt, *Prog. Inorg. Chem.* **1972**, *15*, 201.
[223] G. H. Brauer, *Handbuch der Präparativen Anorganischen Chemie*, *Vol. 1*, 3rd ed., Emke Verlag, Stuttgart, **1975**.
[224] C. J. Schack, D. Pilipovich, *Inorg. Chem.* **1970**, *9*, 1387.
[225] E. H. Appelmann, L. J. Basile, H. Kim, *Inorg. Chem.* **1982**, *21*, 2801.
[226] M. Schmeisser, W. Eckermann, K. P. Gundlach, D. Naumann, *Z. Naturforsch.* **1980**, *35b*, 1143.
[227] W. Gombler, H. Willner, *J. Phys. Edu. Sci. Instrum.* **1987**, *20*, 1286.
[228] H. S. P. Müller, H. Willner, *Inorg. Chem.* **1992**, *31*, 2527.
[229] D. Scheffler, H. Willner, *Inorg. Chem.* **1998**, *37*, 4500.
[230] D. Scheffler, Ph.D thesis, Hannover (Hannover), **1999**.

Received: March 22, 2002
Revised: June 20, 2002 [F3966]

  0947-6539/02/0824-5621 $ 20.00+.50/0